Relaxed Bell inequalities with arbitrary measurement dependence for each observer

Citation: Friedman, Andrew S. et al. "Relaxed Bell inequalities with arbitrary measurement dependence for each observer." Physical Review A 99, 1 (January 2019): 012121 © 2019 American Physical Society

As Published: http://dx.doi.org/10.1103/PhysRevA.99.012121

Publisher: American Physical Society

Persistent URL: http://hdl.handle.net/1721.1/120461

Version: Final published version: final published article, as it appeared in a journal, conference proceedings, or other formally published context

Relaxed Bell inequalities with arbitrary measurement dependence for each observer

Andrew S. Friedman,[1,*] Alan H. Guth,[2,†] Michael J. W. Hall,[3,4,‡] David I. Kaiser,[2,§] and Jason Gallicchio[5,‖]

[1]*Center for Astrophysics and Space Sciences, University of California, San Diego, La Jolla, California 92093, USA*

[2]*Center for Theoretical Physics and Department of Physics, Massachusetts Institute of Technology, Cambridge, Massachusetts 02139, USA*

[3]*Centre for Quantum Computation and Communication Technology (Australian Research Council), Centre for Quantum Dynamics, Griffith University, Brisbane, Queensland 4111, Australia*

[4]*Department of Theoretical Physics, Research School of Physics and Engineering, Australian National University, Canberra ACT 0200, Australia*

[5]*Department of Physics, Harvey Mudd College, Claremont, California 91711, USA*

(Received 4 September 2018; published 24 January 2019)

Bell's inequality was originally derived under the assumption that experimenters are free to select detector settings independently of any local "hidden variables" that might affect the outcomes of measurements on entangled particles. This assumption has come to be known as "measurement independence" (also referred to as "freedom of choice" or "settings independence"). For a two-setting, two-outcome Bell test, we derive modified Bell inequalities that relax measurement independence, for either or both observers, while remaining locally causal. We describe the loss of measurement independence for each observer using the parameters M_1 and M_2, as defined by Hall in 2010, and also by a more complete description that adds two new parameters, which we call $\hat{M}_1$ and $\hat{M}_2$, deriving a modified Bell inequality for each description. These "relaxed" inequalities subsume those considered in previous work as special cases, and quantify how much the assumption of measurement independence needs to be relaxed in order for a locally causal model to produce a given violation of the standard Bell-Clauser-Horne-Shimony-Holt (Bell-CHSH) inequality. We show that both relaxed Bell inequalities are tight bounds on the CHSH parameter by constructing locally causal models that saturate them. For any given Bell inequality violation, the new two-parameter and four-parameter models each require significantly less mutual information between the hidden variables and measurement settings than previous models. We conjecture that the new models, with optimal parameters, require the minimum possible mutual information for a given Bell violation. We further argue that, contrary to various claims in the literature, relaxing freedom of choice need not imply superdeterminism.

DOI: 10.1103/PhysRevA.99.012121

I. INTRODUCTION

Bell's theorem remains a hallmark achievement of modern physics [1–5]. Since Bell derived his inequality more than 50 years ago [1], numerous experiments with entangled particles have demonstrated clear violations of Bell's inequality, including several recent, state-of-the-art tests [6–15], each of them consistent with predictions from quantum mechanics. While lending strong empirical support for quantum theory, these tests more directly imply that at least one eminently reasonable assumption required to derive Bell's theorem must fail to hold in the physical world. These include local causality—which stipulates that measurement outcomes at one detector cannot depend on the settings or outcomes at a distant detector—and experimenters' ability to select detector settings freely, independent of any "hidden variables" that might affect the outcomes of measurements.

If one or more assumptions used to derive Bell's theorem are relaxed, this opens up "loopholes" whereby local "hidden-variable" models could remain consistent with all previous Bell-violating experiments [16,17]. It is therefore crucial to address as many loopholes as possible in a single test.

Some of the best-known loopholes include the possibility of signaling or communication between the detectors regarding the settings or measurement outcomes on each side of the experiment (the "locality" loophole [18,19]), and the possibility that some unknown mechanism is taking advantage of detector inefficiency to bias the sample of entangled particles that are detected (the "detection" or "fair-sampling" loophole [20,21]). There has been considerable interest in conducting experiments that close either the locality or detection loopholes [18,19,22–27], culminating in several recent experimental tests that closed both of these loopholes simultaneously [6–10,15].

In addition, Bell's theorem is derived under the assumption that observers have complete freedom to choose detector settings in an experimental test of Bell's inequality. Relaxing this assumption leads to a third, significant loophole. The "measurement-independence" loophole (also known as the "freedom-of-choice" or "settings-independence" loophole) has received the least attention to date, though recent

*asf@ucsd.edu
†guth@ctp.mit.edu
‡michael.hall@griffith.edu.au
§dikaiser@mit.edu
‖jason@hmc.edu

theoretical work indicates that the use of Bell tests to exclude local hidden-variable theories is most vulnerable to this particular loophole [28–34]. This paper builds on recent interest in theoretical models that relax the measurement-independence assumption [28–46], as well as recent experiments that constrain such models [11,13–15,24,34,42,44].

Even if nature does not exploit the measurement-independence loophole, addressing the various assumptions experimentally has significant practical relevance for numerous entanglement-based technologies. These include device-independent quantum key distribution [47–49] along with random-number generation and randomness expansion [50–58]. In particular, a malicious adversary with knowledge of an opponent's devices could conceivably undermine a variety of quantum information schemes by exploiting the measurement-independence loophole [29,36,59–64].

Physicists have constructed theoretical models that can reproduce the quantum singlet-state predictions for measurements on pairs of entangled particles, while obeying local causality, by relaxing the assumption of measurement independence—that is, by partially constraining or predicting observers' selections among choices of detector settings [28,30–32,65]. The amount of freedom reduction required to reproduce the quantum singlet-state correlations can be quite small, as little as $\simeq 14\%$ deviation from free choice, corresponding to just $\sim 1/15$ of a bit of mutual information between the detector settings and the relevant hidden variables. By contrast, for locally causal models that retain measurement independence, 100% of determinism or locality must be given up to reproduce the singlet-state correlations [28,30,31,66,67], with either generation of one full bit of indeterminism [66] or transmission of one full bit of nonlocal signaling [67] being required. Thus the use of Bell experiments to test quantum mechanics—and, by implication, all known quantum-encryption protocols [29]—is particularly susceptible to the measurement-independence loophole.

Whereas previous work has assumed identical relaxation of measurement independence for all parties [30,31] or 100% freedom for one observer and some nonzero measurement dependence for the other [28,32], in this paper we develop a more general framework that can accommodate different amounts of freedom for each observer. Our motivation stems, in part, from recent efforts to address the measurement-independence loophole experimentally. Some recent experiments have made clever use of human-generated choices [13], while others have relied upon real-time astronomical observation of light from distant objects (such as quasars) to determine detector settings [11,14,15]. Although any estimation of possible measurement dependence for either of these techniques would be highly model dependent, it is plausible that they would be susceptible to different amounts of measurement dependence. Future Bell-Clauser-Horne-Shimony-Holt (Bell-CHSH) tests, in which observers select distinct methods for determining settings at their detectors, would then generically fall into the general class we analyze here.

We describe the amount of freedom for each observer by using the parameters M_1 and M_2 introduced by Hall in 2010 [30], and we also introduce a more complete, four-parameter description that includes two new parameters, which we call $\hat{M}_1$ and $\hat{M}_2$. We consider two-setting, two-outcome Bell-CHSH tests, and derive upper bounds on the Bell-CHSH parameter for models that relax measurement independence but maintain local causality, for both the two-parameter and four-parameter descriptions. We further show that previous bounds for situations with relaxed measurement independence obtained by Hall in Refs. [30,31] and by Banik *et al.* in Ref. [32] are special cases of our more general result. Moreover, we show that both of our new bounds are tight, by constructing two-parameter and four-parameter locally causal models that saturate them. These new models have near-optimal (and conjectured to be optimal) mutual information properties.

The paper is organized as follows. In Sec. II, we review the assumptions required for the derivation of Bell's theorem, and in Sec. III, following Refs. [30,31], we introduce a measure, in terms of parameters M_1 and M_2, with which to quantify each observer's measurement dependence (and also M for overall measurement dependence). In Sec. IV, we derive a corresponding two-parameter relaxed Bell inequality. In Sec. V we demonstrate that our inequality is tight, by constructing a local and deterministic model that saturates it. In Sec. VI, we show that, for a given Bell violation, our model requires significantly less mutual information between measurement settings and hidden variables than previous models, and conjecture that it is in fact optimal in this regard. In Sec. VII we introduce a more complete description of measurement dependence that adds two new parameters, $\hat{M}_1$ and $\hat{M}_2$. We generalize our results to a relaxed four-parameter Bell inequality, and demonstrate that it is tight by presenting a locally causal four-parameter model that saturates it. Conclusions are presented in Sec. VIII. In Appendices A and B we present a distinct two-parameter model that interpolates between the models of Refs. [30,32]. We demonstrate that this interpolating model likewise saturates the upper bound of the two-parameter inequality of Sec. IV, though it requires significantly more mutual information between the hidden variables and measurement settings to reproduce the predictions of quantum mechanics than does the model presented in Sec. V. Several steps in the derivation of the four-parameter Bell inequality of Sec. VII are presented in Appendix C, and the construction of our four-parameter model is described in Appendix D.

II. BELL'S THEOREM ASSUMPTIONS

Bell inequalities place restrictions on the statistical correlations between measurements made by two or more observers, under natural assumptions related to local causality and the selection of measurement settings. For the typical case of two observers, Alice and Bob, we denote Alice's measurement setting on a given run as u and Bob's as v, and the outcomes of their measurements as a and b. The statistical correlations between them are then described by a set of joint probability distributions $\{p(a,b|u,v)\}$. To try to account for the correlations within some hidden-variable model, one parametrizes the joint probability distributions in the form

$$p(a,b|u,v) = \int d\lambda\; p(a,b|u,v,\lambda)\; p(\lambda|u,v), \qquad (1)$$

where λ is a (possibly multicomponent) hidden variable that includes among its components any hidden variables that affect the measurement outcomes. Equation (1) follows from Bayes' theorem and the definition of conditional probability. Note that this equation relies on no assumptions regarding whether events associated with λ occur in the past and/or future of various measurements, or even whether λ represents degrees of freedom associated with specific space-time events at all [68–71].

One may constrain Eq. (1) based on additional assumptions regarding locality, determinism, and measurement independence. These assumptions lead to restrictions on the form that the conditional probabilities $p(a, b, |u, v, \lambda)$ may take [1–5,31,64,68]. The first assumption concerns *local causality*:

$$p(a, b|u, v, \lambda) = p(a|u, \lambda)\, p(b|v, \lambda). \tag{2}$$

Equation (2) assumes the probabilities factorize such that the measurement outcomes on each side depend only on the detector settings on that side and λ. Equation (2) may be derived from the joint assumptions of "outcome independence" and "parameter independence" [68], and is motivated by the theoretical and empirical success of relativity. In an ideal Bell test, each measurement event is spacelike separated from the setting choice and outcome on the other side, and hence cannot be influenced by them if relativistic causality is valid.

The assumption of *determinism* states that the measurement outcomes $a, b \in \{-1, 1\}$ are given by deterministic functions $a = A(u, \lambda)$ and $b = B(v, \lambda)$ of the detector settings and λ. Models with locally causal, deterministic outcomes satisfy

$$p(a|u, \lambda) = \delta_{a,A(u,\lambda)}, \quad p(b|v, \lambda) = \delta_{b,B(v,\lambda)}, \tag{3}$$

where $\delta_{a,A(u,\lambda)}$ and $\delta_{b,B(v,\lambda)}$ are Kronecker delta functions. Determinism thus requires that the conditional outcome probabilities $p(a|u, \lambda)$ and $p(b|v, \lambda)$ must be either 0 or 1. As demonstrated in Ref. [31], any locally causal model that satisfies Eq. (2) for which the outcome probabilities are stochastic (rather than deterministic) functions of the detector setting and λ may be written in the form of a deterministic model with the same degree of measurement dependence M, where M is defined below, in Eq. (8). Hence we restrict attention here to deterministic locally causal models without loss of generality.

Lastly, Alice and Bob must select detector settings. The assumption known variously as *measurement independence*, *settings independence*, or *freedom of choice* stipulates that the choice of joint detector settings (u, v) is independent of λ, which includes in its components all the hidden variables that affect measurement outcomes:

$$p(u, v|\lambda) = p(u, v), \tag{4}$$

which is equivalent (via Bayes's theorem) to the expression

$$p(\lambda|u, v) = p(\lambda). \tag{5}$$

Equations (4) and (5) imply that Alice's and Bob's choice of detector settings will not be affected by the value of λ, and (conversely) that learning Alice's and Bob's detector settings gives no information about the underlying variable λ [24,28–33,33–36,38,39,41–44,64,72,73]. In particular, if Eqs. (4) and (5) hold, then no hidden third party with the power to affect measurement outcomes can nudge the selections for u and/or v on a given experimental run, or gain information about these selections from knowledge or manipulation of λ. We emphasize that these restrictions on third-party influences hold regardless of whether we are considering influences that might be causal, retrocausal [69–71], or represent degrees of freedom that are not associated with specific events in space-time [68].

III. QUANTIFYING MEASUREMENT INDEPENDENCE

In this paper we retain the assumption of local causality (and, without loss of generality, determinism), but relax the assumption of measurement independence. We follow the framework established in Refs. [30,31] to quantify the degree of relaxation. In particular, we use the variational distance between probability distributions for different settings, u and v.

To motivate this, note from Eq. (5) that measurement dependence corresponds to dependence of the hidden-variable distribution $p(\lambda|u, v)$ on u and/or v, Alice and/or Bob's measurement settings. That is, measurement dependence corresponds to $p(\lambda|u_1, v_1) \neq p(\lambda|u_2, v_2)$ for at least some choice of u_1, u_2, v_1, v_2. A well-known way to quantify the difference between two probability distributions $p(\lambda)$ and $q(\lambda)$ is via the variational or trace distance [74,75], which can be defined as

$$D(p, q) \equiv \int d\lambda\, |p(\lambda) - q(\lambda)|. \tag{6}$$

This distance has a simple operational interpretation in terms of an experiment in which one is given a single sample λ drawn with equal probability from either the distribution p or the distribution q, and then asked which probability distribution was used. The probability that one can successfully identify the probability distribution, before knowing the value of λ that was drawn, is given by [74,75]

$$P_{\text{distinguish}} = \tfrac{1}{2}\big[1 + \tfrac{1}{2} D(p, q)\big]. \tag{7}$$

Thus, measurement dependence corresponds to a nonzero distance between $p(\lambda|u_1, v_1)$ and $p(\lambda|u_2, v_2)$ for at least some settings u_1, u_2, v_1, v_2, or, equivalently, to a better than 50:50 chance of distinguishing between the measurement settings (u_1, v_1) and (u_2, v_2) on the basis of learning the value of λ.

We assume that Alice may select her settings from some set U, and Bob from some set V. Then we may define the overall degree of measurement dependence by

$$M \equiv \sup_{u_1,u_2\in U, v_1,v_2\in V} \left\{ \int d\lambda |p(\lambda|u_1, v_1) - p(\lambda|u_2, v_2)| \right\}. \tag{8}$$

It follows that M quantifies the dependence of the hidden variable distribution on the measurement setting via the maximum distance that can be achieved by varying the settings. Further, $\frac{1}{2}(1 + \frac{1}{2}M)$ determines the maximum probability for distinguishing between pairs of measurement settings. For example, if $M = 0$ then there is no measurement dependence: $p(\lambda|u_1, v_1) = p(\lambda|u_2, v_2)$ for all settings (u_1, v_1), (u_2, v_2), and the probability of distinguishing one settings pair from another, based on a sample of λ, is never better than $\frac{1}{2}$. Thus, the hidden variable contains zero information about the measurement settings. Conversely, if $M = 2$, then there

are measurement settings (u_1, v_1) and (u_2, v_2) which can be distinguished with probability one, corresponding to a maximum degree of measurement dependence.

More generally, note that $0 \leqslant M \leqslant 2$. Measurement independence, with $p(\lambda|u, v) = p(\lambda)$ for all u, v, yields $M = 0$. The maximum violation of measurement independence, $M = 2$, corresponds to the case in which two normalized probability distributions $p(\lambda|u_1, v_1)$ and $p(\lambda|u_2, v_2)$ have no overlapping support for any value of λ. In that case, for each λ, at most one of the pairs of joint settings (u_1, v_1) and (u_2, v_2) may be selected. This implies that if the observers have decided to consider only the two possibilities of joint settings (u_1, v_1) or (u_2, v_2), then their choice will be completely dictated by the value of λ, leaving them no freedom at all. It is therefore natural to define a corresponding overall degree of freedom of choice F by [30]

$$F \equiv 1 - \frac{M}{2}. \tag{9}$$

We may similarly define one-sided degrees of measurement dependence, M_1 and M_2 [30]:

$$M_1 \equiv \sup_{u_1,u_2\in U, v\in V} \left\{ \int d\lambda |p(\lambda|u_1, v) - p(\lambda|u_2, v)| \right\}, \tag{10}$$

$$M_2 \equiv \sup_{u\in U, v_1,v_2\in V} \left\{ \int d\lambda |p(\lambda|u, v_1) - p(\lambda|u, v_2)| \right\}. \tag{11}$$

Similarly to the case of the overall measurement dependence M, discussed above, the one-sided measure M_1 quantifies the degree of measurement dependence corresponding to variation of Alice's settings, but with Bob's setting held fixed. Thus, for example, a maximum value $M_1 = 2$ implies there are measurement settings (u_1, v) and (u_2, v), differing only in Alice's local setting, which can be distinguished by a (hypothetical) measurement of λ with probability one. A similar interpretation holds for M_2.

Like M, the one-sided parameters are bounded by $0 \leqslant M_1, M_2 \leqslant 2$; the corresponding degrees of individual freedom of choice are given by $F_1 \equiv 1 - M_1/2$ and $F_2 \equiv 1 - M_2/2$. The M quantities obey the inequality chain [30]

$$\max\{M_1, M_2\} \leqslant M \leqslant \min\{M_1 + M_2, 2\}. \tag{12}$$

For experiments in which Alice and Bob each select among two setting choices, we may write $u \in \{x, x'\}$ and $v \in \{y, y'\}$, and the expressions for M, M_1, and M_2 simplify to

$$M_1 = \max \left\{ \int d\lambda |p(\lambda|x, y) - p(\lambda|x', y)|, \right.$$
$$\left. \times \int d\lambda |p(\lambda|x, y') - p(\lambda|x', y')| \right\}, \tag{13}$$

$$M_2 = \max \left\{ \int d\lambda |p(\lambda|x, y) - p(\lambda|x, y')|, \right.$$
$$\left. \times \int d\lambda |p(\lambda|x', y) - p(\lambda|x', y')| \right\}, \tag{14}$$

$$M = \max \left\{ M_1, M_2, \int d\lambda |p(\lambda|x, y) - p(\lambda|x', y')|, \right.$$
$$\left. \times \int d\lambda |p(\lambda|x, y') - p(\lambda|x', y)| \right\}. \tag{15}$$

These expressions are useful for calculating the degrees of measurement dependence for the CHSH scenario in later sections. We will also consider an alternative measure of correlation, the mutual information between the detector settings and λ [28,31], in Sec. VI, and two further parameters related to M_1 and M_2 in Sec. VII.

IV. RELAXED BELL-CHSH INEQUALITY

In the CHSH correlation scenario, Alice and Bob each have two possible measurement settings, $u \in \{x, x'\}$ and $v \in \{y, y'\}$, respectively, each with two corresponding measurement outcomes, $a, b \in \{-1, 1\}$, respectively. Defining the correlation function

$$\langle ab\rangle_{uv} = \sum_{a,b=\pm 1} ab\, p(a, b|u, v), \tag{16}$$

the CHSH correlation parameter is given by the linear combination [2]

$$S = |\langle ab\rangle_{xy} + \langle ab\rangle_{xy'} + \langle ab\rangle_{x'y} - \langle ab\rangle_{x'y'}|. \tag{17}$$

Noting that each expectation value can be at most ± 1, the maximum possible value for S is 4. However, under the assumptions of local causality [Eq. (2)] and measurement independence [Eq. (5)], one finds the Bell-CHSH inequality [2]:

$$S \leqslant 2. \tag{18}$$

By contrast, quantum mechanics predicts a maximum value $S_{QM} = 2\sqrt{2}$ (known as the "Tsirelson bound" [76]) for certain choices of detector settings. Therefore quantum mechanics is incompatible with the conjunction of local causality and measurement independence.

Experiments now routinely measure $S > 2$ to high statistical significance, in clear violation of the Bell-CHSH inequality [6–15,24,44]. The experimental correlations are compatible with quantum predictions. However, alternative models, distinct from quantum mechanics, can also explain the experimental results if one or more of the assumptions leading to Eq. (18) fail to hold.

Here we construct a relaxed Bell-CHSH inequality for models that satisfy both local causality and determinism, but relax the assumption of measurement independence for each observer. For such models, Eqs. (1)–(3) hold but Eqs. (4) and (5) do not. The correlation function of Eq. (16) then takes the form

$$\langle ab\rangle_{uv} = \int d\lambda\, p(\lambda|u, v)\, A(u, \lambda)\, B(v, \lambda). \tag{19}$$

We parametrize the upper bound for the relaxed CHSH-Bell inequality as

$$S \leqslant 2 + V, \tag{20}$$

where the amount of Bell violation, V, will depend on the degree to which measurement independence has been relaxed for Alice and/or Bob. The Tsirelson bound for quantum mechanics, $S_{QM} = 2\sqrt{2}$, corresponds to a violation

$$V_T = 2(\sqrt{2} - 1) \simeq 0.828. \tag{21}$$

We may therefore quantify how much experimental freedom Alice and/or Bob must forfeit in locally causal models in order to match the Tsirelson bound, with $V = V_T$.

For models that obey local causality but relax the overall degree of measurement independence M in Eq. (8), Hall derived the relaxed Bell-CHSH inequality [30,31]

$$S \leqslant 2 + \min\{3M, 2\} \tag{22}$$

and constructed models saturating this bound with $M = M_1 = M_2$. Such symmetric models reproduce the Tsirelson bound for quantum mechanics if $M_1 = M_2 = M = V_T/3 \simeq 0.276$, corresponding to degrees of experimental freedom $F = F_1 = F_2 \simeq 86.2\%$, i.e., to Alice and Bob each losing $\simeq 13.8\%$ experimental freedom. Note that neither observer needs to forfeit 100% freedom in order to reach the Tsirelson bound.

Subsequently, Banik *et al.* considered one-sided models in which one observer's freedom is partially reduced while the other observer retains complete freedom: either $M_1 = M \neq 0$ and $M_2 = 0$ or vice versa [32]. Without loss of generality, we may consider $M_2 = 0$. (The converse case $M_1 = 0$ follows upon switching observer labels for Alice and Bob, $1 \leftrightarrow 2$.) Then, the relaxed Bell-CHSH inequality

$$S \leqslant 2 + M_1 \tag{23}$$

follows, and is saturated by suitable models with $M = M_1$ and $M_2 = 0$ [32]. Such 1-sided models reproduce the quantum-mechanical Tsirelson bound with $M_1 = M = V_T \simeq 0.828$ and $M_2 = 0$ (or vice versa), corresponding to one observer losing $M_1/2 = M/2 \simeq 41.4\%$ freedom. Though such one-sided scenarios require one of the observers to forfeit three times more experimental freedom than in Hall's symmetric case, such models similarly require considerably less than $M_1 = M = 2$ or 100% reduction of freedom in order to reach the Tsirelson bound.

In this section we derive a general upper bound on S for models that relax measurement independence, as described by the parameters $M_1, M_2 \in [0, 2]$, while maintaining local causality. The general two-parameter bound may be written in the form

$$S \leqslant 2 + V_G(M_1, M_2), \tag{24}$$

with

$$V_G(M_1, M_2) = \min\{M_1 + M_2 + \min\{M_1, M_2\}, 2\}. \tag{25}$$

[In Sec. VII we will define two new parameters related to measurement independence, and will describe a four-parameter bound that generalizes Eqs. (24) and (25).] The bound V_G includes the scenarios studied by Hall in Refs. [30,31] and by Banik *et al.* in Ref. [32] as special cases. In particular, Eqs. (24) and (25) reduce to Eq. (22) for the case $M = M_1 = M_2$ (Hall), and to Eq. (23) for the case $M_2 = 0$ (Banik *et al.*). For the general case, we may visualize the amount of measurement dependence required of each observer in order to reproduce the Tsirelson bound of quantum mechanics ($V = V_T$), or the maximal CHSH violation ($V = 2$), as in Fig. 1.

To derive Eqs. (24) and (25), we first recall that we may assume the model is deterministic as per Eq. (3) without loss of generality. Using Eq. (19) to rewrite Eq. (17) for the CHSH

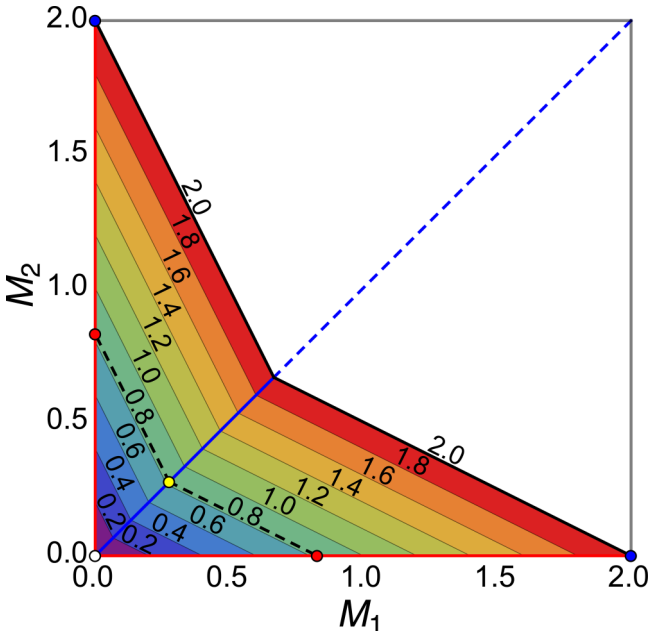

FIG. 1. This "freedom square" indicates the minimum degrees of measurement dependence $M_1, M_2 \in [0, 2]$ required for a locally causal model to predict a given violation V of the Bell-CHSH inequality, as per Eq. (25). Within the region of principal physical interest, with $V = M_1 + M_2 + \min\{M_1, M_2\} \leqslant 2$, contours label the amount of CHSH violation $0 \leqslant V \leqslant 2$. [For $M_1 + M_2 + \min\{M_1, M_2\} > 2$, i.e., the blank region, Eq. (25) yields $V = 2$, corresponding to $S = 4$.] Values of M_1 and M_2 that yield the Tsirelson bound, with $V_T = 2(\sqrt{2} - 1)$, are marked with black dashed lines. The solid black lines mark the boundary of the region that yields maximal CHSH violation, $V = 2$. Symmetric models, like those analyzed in Refs. [30,31], lie along the blue (solid and dashed) diagonal line, with $M_1 = M_2$ [including the light yellow circle at $(M_1, M_2) = (V_T/3, V_T/3)$], while one-sided models, with $M = M_1$ and $M_2 = 0$ or vice versa, as studied in Ref. [32], lie along the M_1 and M_2 axes [including the dark red circles at $(M_1, M_2) = (0, V_T)$ and $(V_T, 0)$]. The original Bell-CHSH inequality corresponds to $V = 0$, and is marked by the white circle at $M_1 = M_2 = 0$.

parameter S then gives

$$\begin{aligned} S = \Big| \int d\lambda [& A(x,\lambda)B(y,\lambda)\, p(\lambda|x,y) \\ & + A(x',\lambda)B(y,\lambda)\, p(\lambda|x',y) \\ & + A(x,\lambda)B(y',\lambda)\, p(\lambda|x,y') \\ & - A(x',\lambda)B(y',\lambda)\, p(\lambda|x',y')] \Big|. \end{aligned} \tag{26}$$

We next use a "plus zero" trick to rewrite Eq. (26) by adding and subtracting identical terms:

$$\begin{aligned} S = \Big| \int d\lambda \{ & p(\lambda|x,y)[A(x,\lambda)B(y,\lambda) + A(x,\lambda)B(y',\lambda)] \\ & + p(\lambda|x',y)[A(x',\lambda)B(y,\lambda) - A(x',\lambda)B(y',\lambda)] \\ & + A(x,\lambda)B(y',\lambda)[p(\lambda|x,y') - p(\lambda|x,y)] \\ & - A(x',\lambda)B(y',\lambda)[p(\lambda|x',y') - p(\lambda|x',y)]\} \Big|. \end{aligned} \tag{27}$$

Upon using the triangle inequality, we conclude that

$$S \leqslant T_1 + T_2 + T_3, \tag{28}$$

with T_1, T_2, and T_3 given by

$$T_1 = \int d\lambda |p(\lambda|x, y)[A(x, \lambda)B(y, \lambda) + A(x, \lambda)B(y', \lambda)] + p(\lambda|x', y)[A(x', \lambda)B(y, \lambda) - A(x', \lambda)B(y', \lambda)]|, \tag{29}$$

$$T_2 = \int d\lambda |A(x, \lambda)B(y', \lambda)[p(\lambda|x, y') - p(\lambda|x, y)]|, \tag{30}$$

and

$$T_3 = \int d\lambda |A(x', \lambda)B(y', \lambda)[p(\lambda|x', y') - p(\lambda|x', y)]|. \tag{31}$$

Since the deterministic outcome functions always have magnitude $|A(x, \lambda)| = |B(y', \lambda)| = 1$, T_2 in Eq. (30) may be simplified:

$$T_2 = \int d\lambda |p(\lambda|x, y') - p(\lambda|x, y)| \leqslant M_2, \tag{32}$$

upon using Eq. (14) for M_2. Similarly,

$$T_3 = \int d\lambda |p(\lambda|x', y') - p(\lambda|x', y)| \leqslant M_2. \tag{33}$$

Next, Eq. (29) for T_1 may be rearranged:

$$T_1 = \int d\lambda |B(y, \lambda)[A(x, \lambda)p(\lambda|x, y) + A(x', \lambda)p(\lambda|x', y)] + B(y', \lambda)[A(x, \lambda)p(\lambda|x, y) - A(x', \lambda)p(\lambda|x', y)]|. \tag{34}$$

Again using the triangle inequality and the fact that $|A(x, \lambda)| = |A(x', \lambda)| = |B(y, \lambda)| = |B(y', \lambda)| = 1$ yields

$$\begin{aligned} T_1 &\leqslant \int d\lambda \left\{ \left| B(y, \lambda)A(x, \lambda) \times \left[p(\lambda|x, y) + \frac{A(x', \lambda)}{A(x, \lambda)} p(\lambda|x', y) \right] \right| \right. \\ &\quad \left. + \left| B(y', \lambda)A(x, \lambda) \left[p(\lambda|x, y) - \frac{A(x', \lambda)}{A(x, \lambda)} p(\lambda|x', y) \right] \right| \right\} \\ &\leqslant \int d\lambda \left\{ \left| p(\lambda|x, y) + \frac{A(x', \lambda)}{A(x, \lambda)} p(\lambda|x', y) \right| \right. \\ &\quad \left. + \left| p(\lambda|x, y) - \frac{A(x', \lambda)}{A(x, \lambda)} p(\lambda|x', y) \right| \right\}. \end{aligned} \tag{35}$$

The quantity $A(x', \lambda)/A(x, \lambda)$ is always equal to $+1$ or -1 for any value of λ. For either choice, one of the absolute-value arguments in Eq. (35) will be $p(\lambda|x, y) + p(\lambda|x', y)$, and the other will be $p(\lambda|x, y) - p(\lambda|x', y)$. Thus Eq. (35) simplifies to

$$T_1 \leqslant \int d\lambda \{ |p(\lambda|x, y) + p(\lambda|x', y)| \tag{36}$$

$$+ |p(\lambda|x, y) - p(\lambda|x', y)| \}. \tag{37}$$

But

$$\int d\lambda |p(\lambda|x, y) + p(\lambda|x', y)| = 2, \tag{38}$$

since the function $p(\lambda|x, y)$ is a normalized conditional probability distribution, and

$$\int d\lambda |p(\lambda|x, y) - p(\lambda|x', y)| \leqslant M_1, \tag{39}$$

upon using Eq. (13). Therefore

$$T_1 \leqslant 2 + M_1. \tag{40}$$

Combining Eqs. (28), (32), (33), and Eq. (40), we find

$$S \leqslant 2 + M_1 + 2M_2. \tag{41}$$

However, since the formalism makes no distinction between the first and second observer's detectors, we can carry out a parallel set of manipulations, reversing the treatment of x and y, to similarly obtain

$$S \leqslant 2 + M_2 + 2M_1. \tag{42}$$

Finally, since S is less than or equal to the right-hand sides of Eqs. (41) and (42), then it must be upper bounded by the minimum of the two, i.e.,

$$S \leqslant 2 + M_1 + M_2 + \min\{M_1, M_2\}. \tag{43}$$

Noting that $S \leqslant 4$ from Eq. (17), we arrive at

$$S \leqslant 2 + \min\{M_1 + M_2 + \min\{M_1, M_2\}, 2\}, \tag{44}$$

which is equivalent to Eqs. (24) and (25), as desired.

V. TIGHTNESS OF THE GENERAL TWO-PARAMETER BOUND

In this section we demonstrate that Eqs. (24) and (25) yield a tight upper bound on the CHSH parameter S for hidden-variable models that obey local causality while relaxing measurement independence, as described by the parameters M_1 and M_2. To do so, it suffices to show that, for each value of M_1 and M_2, at least one model exists that saturates $S = 2 + V_G(M_1, M_2)$, with V_G given by Eq. (25). Hence, similarly to the approach in Refs. [30–32], we will construct model tables with values for Alice's and Bob's measurement outcomes, $A(x, \lambda_i)$ and $B(y, \lambda_i)$, and conditional probabilities for various values of the hidden variable, $p(\lambda_i|x, y)$, subject to the constraint that the $p(\lambda_i|x, y)$ are non-negative and properly normalized. We will nonetheless show in Sec. VII that if we have additional information about a model, in the form of two new parameters, then we can derive a more general four-parameter bound that can sometimes be tighter than the two-parameter bound of Eqs. (24) and (25).

In particular, we consider a model with a hidden variable λ that can take on any of 4 discrete values, $\lambda_1, \lambda_2, \lambda_3, \lambda_4$, as per Tables I and II. For this model the deterministic measurement-outcome functions $A(u, \lambda_i)$ and $B(v, \lambda_i)$, for Alice and Bob, respectively, are of the forms defined in Table I, where the arbitrary constants c, d, e, f may be any values in $\{-1, 1\}$. The conditional probabilities are parametrized by three numbers p_1, p_2, and p_3 as per Table II, that can be set to allow different amounts of Bell violation $V_G(M_1, M_2)$ via Eq. (25) consistent

TABLE I. Deterministic measurement-outcome functions $A(u, \lambda_i)$ and $B(v, \lambda_i)$ for Alice's and Bob's measurements, given λ_i with $i = 1, \ldots, 4$. The values of the measurement outcomes (c, d, e, f) are selected arbitrarily from $\{-1, 1\}$.

λ_i	$A(x, \lambda)$	$A(x', \lambda)$	$B(y, \lambda)$	$B(y', \lambda)$
λ_1	c	c	c	c
λ_2	d	$-d$	d	d
λ_3	e	e	e	$-e$
λ_4	f	$-f$	$-f$	f

with $S = 2 + V_G(M_1, M_2)$ from Eq. (24), for different values of M_1, M_2.

The correlations between Alice and Bob's outcomes can be determined from Tables I and II via Eq. (19), and we find the CHSH parameter S of Eq. (17) takes the form

$$S = 2 + 2p_1 + 4p_2 - 4p_3. \tag{45}$$

Provided that $p_1 \geqslant p_2 \geqslant p_3$, the degrees of measurement dependence M_1 and M_2 follow via Eqs. (13) and (14) as

$$M_1 = \max\{2p_1, 2p_1\} = 2p_1, \tag{46}$$

$$M_2 = \max\{2p_2, 2p_2\} = 2p_2. \tag{47}$$

(For this model, we also find $M = \max\{M_1, M_2\} = M_1$.)

For arbitrary $M_1 \geqslant M_2$ in the range $0 \leqslant M_1 \leqslant 2$, $0 \leqslant M_2 \leqslant 2$, it follows that if we choose

$$\begin{aligned} p_1 &= M_1/2, \\ p_2 &= M_2/2, \\ p_3 &= \begin{cases} 0, & \text{if } M_1 + 2M_2 \leqslant 2, \\ \frac{1}{4}(M_1 + 2M_2 - 2), & \text{otherwise,} \end{cases} \end{aligned} \tag{48}$$

in Table II, then the constraints $p_1 \geqslant p_2 \geqslant p_3$ are satisfied, and Eq. (45) simplifies to

$$S = \begin{cases} 2 + M_1 + 2M_2, & \text{if } M_1 + 2M_2 \leqslant 2, \\ 4, & \text{otherwise.} \end{cases} \tag{49}$$

Furthermore, one can check that for these values of p_1, p_2, and p_3, all the conditional probabilities in Table II are non-negative. It follows that, with this choice, the local deterministic model corresponding to Table II saturates the relaxed Bell inequality in Eq. (24) for all values $M_1 \geqslant M_2$.

TABLE II. Conditional probabilities $p(\lambda_i|u, v)$ for the value of the hidden variable λ to be λ_i, for $M_1 \geqslant M_2$. Normalization may by checked by summing the entries in each column. The probabilities must be non-negative, and we will see after Eqs. (48) that the entries are non-negative for the entire range of allowed values of (M_1, M_2).

λ_i	$p(\lambda\|x, y)$	$p(\lambda\|x, y')$	$p(\lambda\|x', y)$	$p(\lambda\|x', y')$
λ_1	$\frac{1+p_1+2p_3}{4}$	$\frac{1+p_1-2p_3}{4}$	$\frac{1-p_1+2(p_2-p_3)}{4}$	$\frac{1-p_1-2(p_2-p_3)}{4}$
λ_2	$\frac{1+p_1-2p_3}{4}$	$\frac{1+p_1+2p_3}{4}$	$\frac{1-p_1-2(p_2-p_3)}{4}$	$\frac{1-p_1+2(p_2-p_3)}{4}$
λ_3	$\frac{1-p_1+2(p_2-p_3)}{4}$	$\frac{1-p_1-2(p_2-p_3)}{4}$	$\frac{1+p_1+2p_3}{4}$	$\frac{1+p_1-2p_3}{4}$
λ_4	$\frac{1-p_1-2(p_2-p_3)}{4}$	$\frac{1-p_1+2(p_2-p_3)}{4}$	$\frac{1+p_1-2p_3}{4}$	$\frac{1+p_1+2p_3}{4}$

Finally, by symmetry, one may construct equivalent tables for the case $M_2 \geqslant M_1$, by switching settings labels $x \leftrightarrow y$, $x' \leftrightarrow y'$ and subscripts $1 \leftrightarrow 2$ in Table II. We have therefore demonstrated that the two-parameter upper bound derived in Eq. (25) is a tight upper bound, in the sense that no better bound depending only on M_1 and M_2 is possible.

It is worth noting that while the model in Tables I and II saturates the Hall and Banik *et al.* relaxed Bell inequalities in Eqs. (22) and (23), for the respective special cases $M_1 = M_2$ and $M_2 = 0$, the model of this section is very different from those in Table I of Ref. [30] and Table 1 of Ref. [32]. An alternative saturating model for arbitrary M_1 and M_2, that interpolates between the Hall and the Banik *et al.* models, is given in Appendix A. However, as will be seen below, the model in Tables I and II has significantly better mutual information properties.

VI. MUTUAL INFORMATION PROPERTIES AND COMPARISONS

The degrees of measurement dependence, M_1, M_2, and M, quantify the correlation of the hidden variables λ with Alice's settings and/or Bob's settings. One may alternatively quantify the correlation in terms of the corresponding mutual information [28,31], which has a more direct interpretation as the average information that may be obtained about one variable from knowledge of the other. In this section we calculate the mutual information required to achieve a violation V of the CHSH inequality for the model in Tables I and II. We conjecture that this model is in fact optimal in the sense of requiring the lowest possible mutual information for a given violation V.

A. Calculating mutual information

The mutual information between the hidden variable λ and the joint measurement setting (u, v), measured in units of bits, is given by

$$\begin{aligned} I &\equiv \sum_{\lambda,u,v} p(\lambda, u, v) \log_2 \frac{p(\lambda, u, v)}{p(\lambda)p(u, v)} \\ &= \sum_{\lambda,u,v} p(\lambda|u, v)p(u, v) \log_2 \frac{p(\lambda|u, v)}{p(\lambda)}, \end{aligned} \tag{50}$$

where $p(u, v)$ is the probability distribution of joint measurement settings and $p(\lambda, u, v) \equiv p(\lambda|u, v)p(u, v)$. Note that the mutual information vanishes identically in the case of measurement independence, for which $p(\lambda|u, v) = p(\lambda)$ as per Eq. (5).

We will calculate the mutual information, using Eq. (50), for the standard CHSH scenario in which the settings are chosen randomly and independently of each other (though not independently of the hidden variable). For this scenario, $p(u, v) = 1/4$ for each settings pair, and the mutual information for the saturating model of the previous section simplifies to

$$I_G = H_\Lambda - \tfrac{1}{4}(H_{xy} + H_{xy'} + H_{x'y} + H_{x'y'}), \tag{51}$$

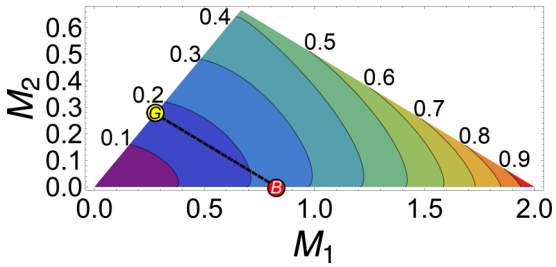

FIG. 2. "Freedom square" plot for the region $V_G(M_1, M_2) = M_1 + 2M_2 \leqslant 2$, $M_1 \geqslant M_2$, labeled by contours of mutual information $I_G(M_1, M_2) \in [0, 1]$ in bits from Eq. (54). The dashed line is the slice corresponding to the Tsirelson bound, $V_G(M_1, M_2) = V_T$, and connects the case $(M_1, M_2) = (V_T, 0)$ [dark red circle for the Banik *et al.* model (B)] to the case $(M_1, M_2) = (V_T/3, V_T/3)$ [light yellow circle (G)]. Relevant cases are explored further in Fig. 3. The line $M_1 = M_2$ minimizes the mutual information for the general saturating model in Tables I and II, for each value of Bell violation $V \in [0, 2]$ [see also Eqs. (57)–(58) and Fig. 3].

where

$$H_\Lambda \equiv -\sum_{i=1}^{4} p(\lambda_i) \log_2 p(\lambda_i) \tag{52}$$

and

$$H_{uv} \equiv -\sum_{i=1}^{4} p(\lambda_i|u, v) \log_2 p(\lambda_i|u, v) \tag{53}$$

denote the entropies of the distributions $p(\lambda)$ and $p(\lambda|u, v)$, respectively. Note that for $p(u, v) = 1/4$, we have $p(\lambda_i) = \sum_{u,v} p(u, v)p(\lambda_i|u, v) = \frac{1}{4}\sum_{u,v} p(\lambda_i|u, v)$.

As per Table II, we consider the case $M_1 \geqslant M_2$, and restrict attention to the range $M_1 + 2M_2 \leqslant 2$ with $p_3 = 0$. Then the CHSH inequality becomes $S \leqslant 2 + V_G(M_1, M_2) = 2 + M_1 + 2M_2$. This covers the whole range of possible violations $V \in [0, 2]$. (As before, the case $M_2 \geqslant M_1$ follows upon switching observer labels.)

It follows, using Table II and Eq. (51), and taking $p_1 = M_1/2$, $p_2 = M_2/2$, $p_3 = 0$ as per Eq. (48), that the mutual information is given by

$$I_G(M_1, M_2) = \frac{1}{4}\left\{2h\left(1 + \frac{M_1}{2}\right) + h\left(1 - \frac{M_1}{2} + M_2\right) + h\left(1 - \frac{M_1}{2} - M_2\right)\right\}, \tag{54}$$

where

$$h(x) \equiv x \log_2(x). \tag{55}$$

Equation (54) for $I_G(M_1, M_2)$ is depicted in Fig. 2.

B. Comparison with previous models

To gain further insight, and to make comparisons with previous work, it is of interest to consider the behavior of $I_G(M_1, M_2)$ for a given degree of violation $V = M_1 + 2M_2$ (e.g., the maximum quantum violation V_T corresponding to the dashed line in Fig. 2). For example, is the amount of mutual information minimized by choosing $M_1 = M_2$ (the yellow circle in Fig. 2 for $V = V_T$), or by choosing $M_1 = V$, $M_2 = 0$ (the red circle in Fig. 2 for $V = V_T$)? And how does this minimum mutual information compare with the corresponding values for the Hall and the Banik *et al.* models in Refs. [30,32]?

First, using the relation $M_1 = V - 2M_2 \geqslant M_2$, we express Eq. (54) in terms of M_2 and the amount of violation V:

$$\tilde{I}_G(V, M_2) \equiv I_G(V - 2M_2, M_2) = \frac{1}{4}\left\{2h\left(1 + \frac{V}{2} - M_2\right) + h\left(1 - \frac{V}{2} + 2M_2\right) + h\left(1 - \frac{V}{2}\right)\right\}, \tag{56}$$

with M_2 restricted to the range $0 \leqslant M_2 \leqslant V/3 \leqslant 2/3$. It is then straightforward to minimize this quantity with respect to M_2, for any given value of the violation V, leading to the result

$$\tilde{I}_G(V) \equiv \min_{M_2} \tilde{I}_G(V, M_2) = I_G(V/3, V/3) = \frac{1}{4}\left\{3h\left(1 + \frac{V}{6}\right) + h\left(1 - \frac{V}{2}\right)\right\}, \tag{57}$$

where the minimum is achieved for the values

$$M_1 = M_2 = M = \frac{V}{3}. \tag{58}$$

By comparison, the Hall model from Table I of Ref. [30] (see also Appendix A) has a corresponding mutual information

$$I_H(V) = \frac{V}{2} \log_2 \frac{4}{3}, \tag{59}$$

for a given degree of violation V, while the Banik *et al.* model from Table 1 of Ref. [32] (see also Appendix A) has a corresponding mutual information

$$I_B(V) = \tfrac{1}{4}\{6 + 2h(2 - V) - h(4 - V)\}. \tag{60}$$

Equations (57), (59), and (60) are plotted as functions of V in Fig. 3, showing that

$$\tilde{I}_G(V) < I_H(V) < I_B(V) \tag{61}$$

for all $V \in (0, 2)$.

As an example, consider the case of the maximum quantum violation $V = V_T$, depicted by colored circles in Fig. 3. While the Hall model requires a mutual information $I_H(V_T) \approx 0.172$ bits [green circle (H)], which is less than the $I_B(V_T) \approx 0.247$ bits required by the Banik model [red circle (B)], the general model of Table II can achieve the maximum quantum violation with a substantially smaller mutual information,

$$\tilde{I}_G(V_T) = \frac{1}{4}\left\{3h\left(\frac{2 + \sqrt{2}}{3}\right) + h(2 - \sqrt{2})\right\} \approx 0.0462738 \text{ bits}, \tag{62}$$

[yellow circle (G)], corresponding via Eqs. (21) and (58) to

$$M_1 = M_2 = \frac{V_T}{3} = \frac{2}{3}(\sqrt{2} - 1). \tag{63}$$

Hence, the model in Table II requires significantly less mutual information between the settings and hidden variables to

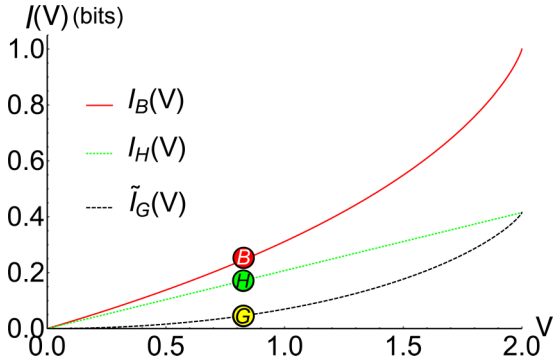

FIG. 3. Mutual information for the Banik *et al.* model [$I_B(V)$, solid red curve], the Hall model [$I_H(V)$, dotted green curve] from the literature [30,32], and the minimum of the general model [$\tilde{I}_G(V)$, dashed black curve] in bits, plotted as a function of CHSH violation $V \in [0, 2]$. As in Fig. 2, large filled circles denote $V_G(M_1, M_2) = V_T$. Note that since $\tilde{I}_G(V) < I_H(V) < I_B(V)$ for all violations $0 < V < 2$, the Hall model always requires less mutual information than the Banik model to produce a given Bell violation, while the minimum of the general model requires much less mutual information than the Hall or Banik models.

simulate violations of the Bell-CHSH inequality than previously studied locally causal models.

In Appendix A we construct an alternative model which also saturates the the general two-parameter bound in Eqs. (24) and (25) for arbitrary values of M_1 and M_2, which is a simple mixture of the Hall and Banik *et al.* models. As is shown in Appendix B, this mixed model is interesting in that it requires less mutual information than either the Hall or Banik models for a given violation V. However, it nevertheless requires significantly more mutual information than the model in Table II.

C. An optimality conjecture

Remarkably, the value of $\tilde{I}_G(V_T) \approx 0.0462738 \sim 1/22$ of a bit in Eq. (62) is *identical* to the mutual information reported in Eq. (37) of Ref. [31], where the latter is for the local deterministic model of general singlet-state correlations given in Ref. [30] when restricted to the CHSH scenario with detector angles chosen to maximize the quantum prediction for the Bell inequality violation. The underlying reason for this agreement is that the hidden variable λ for the singlet-state model is represented by a point on the unit sphere, with its relation to the CHSH measurement settings wholly determined by which one of four regions of the sphere that it lies in. In particular, these regions generate four sets of conditional probabilities that correspond to the rows of Table II for M_1 and M_2 in Eq. (63).

The full singlet-state model in Ref. [30] has a high degree of symmetry, and requires the lowest known mutual information by far of any such model when arbitrary numbers of measurement settings are allowed on each side [30,64]. Hence, given that the saturating model in Table II is similarly highly symmetric for all $M_1 = M_2$ (and $p_3 = 0$), and requires significantly lower mutual information than other known models for general values of V, we conjecture that $\tilde{I}_G(V)$ is in fact the minimum amount of mutual information required for any locally causal model of a given Bell-CHSH violation V.

VII. GENERALIZING FROM TWO PARAMETERS TO FOUR PARAMETERS

So far we have been describing the degree of measurement dependence of Alice and Bob by the traditional parameters [30] M_1 and M_2, as defined in general by Eqs. (10) and (11), and specifically for the CHSH scenario by Eqs. (13) and (14). There are, however, other interesting variables that can be defined by

$$\hat{M}_1 \equiv \inf_{v\in V}\left\{\sup_{u_1,u_2\in U}\left[\int d\lambda |p(\lambda|u_1, v) - p(\lambda|u_2, v)|\right]\right\}, \tag{64}$$

$$\hat{M}_2 \equiv \inf_{u\in U}\left\{\sup_{v_1,v_2\in V}\left[\int d\lambda |p(\lambda|u, v_1) - p(\lambda|u, v_2)|\right]\right\}. \tag{65}$$

These quantities also have a relevant physical interpretation. M_1 describes the most serious loss of freedom that Alice (who sets detector 1) might experience, but the actual loss of freedom that she will experience depends on the value of v, the setting on the other side. For the general case of Eq. (10), the probability that she experiences this worst-case scenario might be extremely small, if the setting v that maximizes the expression is extremely improbable. For example, a model might have the property that Alice can make only one choice if the angle on the far side is between 22 degrees and $22 + 10^{-500}$ degrees, but otherwise she is completely unrestricted. In this case M_1 would be equal to its maximal value of 2, even though the restrictions on Alice's choices are so rare that they could never be detected in the lifetime of many universes.

The quantity $\hat{M}_1$, by contrast, describes the inevitable, minimum loss of freedom that Alice will experience, no matter what value the setting v has. For the example just discussed, $\hat{M}_1$ would equal zero. $\hat{M}_1$ could of course also be misleading, since again the setting v that minimizes the expression in Eq. (64) might be extremely improbable. Nonetheless, we can always count on $\hat{M}_1$ and M_1 to bracket the degree of measurement dependence that Alice will experience. In the context of our two-setting CHSH Bell test, the difference between $\hat{M}_1$ and $\hat{M}_2$ and the usual M_1 and M_2 is the choice between taking the min or the max of the two quantities on the right-hand side of Eqs. (13) and (14).

Finally, we may also interpret $\hat{M}_1$ in terms of an experiment in which one tries to use a measurement of λ to distinguish between two of Alice's measurement settings, with Bob's setting the same in both cases. Varying over Bob's setting and Alice's two settings, the minimum value of the probability that one will be able to identify Alice's setting is given by $\frac{1}{2}(1 + \frac{1}{2}\hat{M}_1)$ (see Sec. III). A similar interpretation applies to $\frac{1}{2}(1 + \frac{1}{2}\hat{M}_2)$.

A. The general four-parameter bound

If we reexamine the proof of the general two-parameter bound in Sec. IV, we find that it leads not only to the two-parameter bound of Eq. (44), but also to a more detailed four-parameter bound, based on M_1, M_2, $\hat{M}_1$, and $\hat{M}_2$. To see this, start by noticing that the quantities T_2 and T_3, defined in Eqs. (32) and (33), are identical to the two quantities

appearing inside the curly brackets in the expression for M_2 in Eq. (14). The larger of these two quantities becomes M_2, but the smaller becomes $\hat{M}_2$, as can be seen from the definition in Eq. (65). Thus,

$$T_2 + T_3 = M_2 + \hat{M}_2. \tag{66}$$

From Eqs. (37)–(40), we can conclude that

$$T_1 \leqslant 2 + M_1[y], \tag{67}$$

where we introduce the definitions

$$M_1[v] \equiv \int d\lambda |p(\lambda|x, v) - p(\lambda|x', v)|, \tag{68}$$

$$M_2[u] \equiv \int d\lambda |p(\lambda|u, y) - p(\lambda|u, y')|, \tag{69}$$

where $u \in \{x, x'\}$ and $v \in \{y, y'\}$. But there is nothing about this system that makes any absolute distinction between y and y', so one could have constructed a rearrangement of the derivation shown, in which y' would appear in Eqs. (37)–(40), instead of y. Then, in addition to Eq. (67), we would also have

$$T_1 \leqslant 2 + M_1[y']. \tag{70}$$

From Eqs. (67) and (70), we conclude that

$$T_1 \leqslant 2 + \hat{M}_1, \tag{71}$$

and then finally

$$S \leqslant 2 + M_2 + \hat{M}_2 + \hat{M}_1. \tag{72}$$

The claim that we can interchange y and y' is not completely obvious, because the definition of S, in Eq. (17), is not invariant under $y \leftrightarrow y'$. The change in S, however, can be compensated by redefinitions of the outcome variables b and b', so the result shown in Eq. (70) is correct. Probably the easiest way to show this clearly is to explicitly construct the rearrangement of the original derivation, which we do in Appendix C, to derive Eq. (70).

Now, following the original derivation in Sec. IV, we use the fact that the formalism makes no distinction between the first and second observer's detectors, so we can carry out a parallel derivation reversing the treatment of x and y, and hence 1 and 2, showing that

$$S \leqslant 2 + M_1 + \hat{M}_1 + \hat{M}_2. \tag{73}$$

Since Eqs. (72) and (73) are both valid inequalities, S must be bounded by the smaller of the two, and of course it must be bounded by 4. So, finally,

$$S \leqslant 2 + \min\{\hat{M}_1 + \hat{M}_2 + \min\{M_1, M_2\},\ 2\}. \tag{74}$$

We will refer to this equation as the general four-parameter bound.

Note that the general four-parameter bound immediately implies the general two-parameter bound of Eq. (44), since $\hat{M}_1 \leqslant M_1$ and $\hat{M}_2 \leqslant M_2$. But, for any model where $\hat{M}_1 \neq M_1$ or $\hat{M}_2 \neq M_2$, the four-parameter bound will be tighter than the two-parameter bound. This statement, of course, does not contradict our previous statement that the two-parameter bound is tight; it is tight, in the sense that it is not possible to have a more stringent bound that depends only on the parameters M_1 and M_2. But with the additional information involved in specifying $\hat{M}_1$ and $\hat{M}_2$, the more stringent bound of Eq. (74) can be established.

B. Saturating the four-parameter bound

Given that the general four-parameter bound is more stringent than the two-parameter bound, we should ask whether the four-parameter bound is tight. We follow the same procedure that we used in Sec. V, showing in this case that for each allowed value of $(M_1, M_2, \hat{M}_1, \hat{M}_2)$, at least one consistent model exists that saturates the bound.

In this case the construction of the model is more complicated. The model described in Tables I and II was found essentially by trial and error, but it is much harder when there are four independent parameters. However, by examining the proof of the bound, step by step, it is possible to list exactly what properties the conditional probabilities must obey for the bound to be saturated. These properties do not determine the conditional probabilities uniquely, but they constrain the system enough so that we were then able to use trial and error methods to construct a general four-parameter model, for any allowed $(M_1, M_2, \hat{M}_1, \hat{M}_2)$, which saturates the bound and thereby proves that the bound is tight: it is not possible to have a more stringent bound that depends only on the parameters M_1, M_2, $\hat{M}_1$, and $\hat{M}_2$. The four-parameter model that we will present has the property that it reduces to the two-parameter model of Tables I and II when $\hat{M}_1 \to M_1$ and $\hat{M}_2 \to M_2$. Here we describe the four-parameter model, and in Appendix D we will summarize the details of the construction.

The allowed range of variables is of course restricted by

$$M_1, M_2, \hat{M}_1, \hat{M}_2 \in [0, 2],\ \hat{M}_1 \leqslant M_1,\ \hat{M}_2 \leqslant M_2, \tag{75}$$

but with four parameters there is also a triangle inequality that limits the amount by which M_1 and $\hat{M}_1$ can differ, and similarly for M_2 and $\hat{M}_2$. Specifically,

$$\begin{aligned} M_1 &= \sum_{i=1}^{4} |p(\lambda_i|x, y) - p(\lambda_i|x', y)| \\ &= \sum_{i=1}^{4} |[p(\lambda_i|x, y) - p(\lambda_i|x, y')] \\ &\quad + [p(\lambda_i|x, y') - p(\lambda_i|x', y')] \\ &\quad + [p(\lambda_i|x', y') - p(\lambda_i|x', y)]| \\ &\leqslant \sum_{i=1}^{4} |[p(\lambda_i|x, y) - p(\lambda_i|x, y')]| \\ &\quad + |[p(\lambda_i|x, y') - p(\lambda_i|x', y')]| \\ &\quad + |[p(\lambda_i|x', y') - p(\lambda_i|x', y)]| \\ &= M_2 + \hat{M}_1 + \hat{M}_2. \end{aligned} \tag{76}$$

There is a parallel identity that can be derived by interchanging 1 and 2, so we have

$$M_1 - \hat{M}_1 \leqslant M_2 + \hat{M}_2, \quad M_2 - \hat{M}_2 \leqslant M_1 + \hat{M}_1. \tag{77}$$

Equations (75) and (77) define the allowed range of variables, except that we will also, without loss of generality, adopt the convention that $M_1 \geqslant M_2$. (If this is not the case, the labels 1 and 2 can be interchanged.)

TABLE III. Conditional probabilities $p(\lambda_i|u,v)$ for the value of the hidden variable λ to be λ_i, for $M_1 \geqslant M_2$ and $M_2+\hat{M}_1+\hat{M}_2 \leqslant 2$.

λ_i	$p(\lambda\|x,y)$	$p(\lambda\|x,y')$	$p(\lambda\|x',y)$	$p(\lambda\|x',y')$
λ_1	$q_1+\frac{1}{4}(M_2+\hat{M}_1+q_2)$	$q_1+\frac{1}{4}(M_2+\hat{M}_1-q_2)$	$q_1+\frac{1}{2}(-M_1+\hat{M}_1+\hat{M}_2+q_2)$	q_1
λ_2	$q_1+\frac{1}{4}(-M_2+\hat{M}_1+2\hat{M}_2+q_2)$	$q_1+\frac{1}{4}(-M_2+\hat{M}_1+2\hat{M}_2+q_2)$	q_1	$q_1+\frac{1}{2}\hat{M}_2$
λ_3	$q_1+\frac{1}{2}(M_2-q_2)$	q_1	$q_1+\frac{1}{4}(2M_1+M_2-\hat{M}_1-3q_2)$	$q_1+\frac{1}{4}(M_2+\hat{M}_1-q_2)$
λ_4	q_1	$q_1+\frac{1}{2}M_2$	$q_1+\frac{1}{4}(M_2+\hat{M}_1+q_2)$	$q_1+\frac{1}{4}(M_2+\hat{M}_1+q_2)$

Table I can be used again, but we need a new table of conditional probabilities to replace Table II. In principle one table of conditional probabilities would suffice, but the individual entries become rather complicated, so we instead first introduce Table III, which describes the model only for the restricted case of $M_2+\hat{M}_1+\hat{M}_2 \leqslant 2$.

Here

$$q_1 \equiv \tfrac{1}{8}(2-M_2-\hat{M}_1-\hat{M}_2), \tag{78}$$

$$q_2 \equiv \min(M_1-\hat{M}_1, M_2). \tag{79}$$

When $M_2+\hat{M}_1+\hat{M}_2 > 2$, there are additional terms that need to be added, as shown in Table IV.

The functions q_3 and q_4 vanish for $M_2+\hat{M}_1+\hat{M}_2 \leqslant 2$, and they are given in general by

$$q_3 = \begin{cases} 0, & \text{if } M_2+\hat{M}_1+\hat{M}_2 \leqslant 2, \\ \frac{1}{8}[M_2+\hat{M}_1+\hat{M}_2-2], & \text{otherwise,} \end{cases} \tag{80}$$

$$q_4 = \begin{cases} 0, & \text{if } M_2+\hat{M}_1+\hat{M}_2 \leqslant 2, \\ \frac{1}{4}[-2-\hat{M}_1-\hat{M}_2 & \\ +\min(M_1+\hat{M}_2, 2) & \\ +\max(M_2+\hat{M}_1, 2)-q_2], & \text{otherwise.} \end{cases} \tag{81}$$

For $M_2+\hat{M}_1+\hat{M}_2 > 2$, the function q_4 can also be written as

$$\tfrac{1}{4}[\max(\bar{R}-R, M_2)+\max(R, \hat{M}_2)-\max(\bar{R}, M_2)-\hat{M}_2], \tag{82}$$

where

$$R \equiv M_2+\hat{M}_1+\hat{M}_2-2, \quad \bar{R} \equiv M_1+M_2+\hat{M}_2-2, \tag{83}$$

TABLE IV. Conditional probabilities $p(\lambda_i|u,v)$ for the value of the hidden variable λ to be λ_i, for any allowed values of M_1, M_2, $\hat{M}_1$, and $\hat{M}_2$, provided that $M_1 \geqslant M_2$. Here $P^{(0)}_{i,j}$ refers to the corresponding entries of Table III.

λ_i	$p(\lambda\|x,y)$	$p(\lambda\|x,y')$	$p(\lambda\|x',y)$	$p(\lambda\|x',y')$
λ_1	$P^{(0)}_{1,1}+q_3$	$P^{(0)}_{1,2}-q_3-q_4$	$P^{(0)}_{1,3}-q_3+q_4$	$P^{(0)}_{1,4}+q_3$
λ_2	$P^{(0)}_{2,1}-q_3+q_4$	$P^{(0)}_{2,2}+q_3+2q_4$	$P^{(0)}_{2,3}+q_3$	$P^{(0)}_{2,4}-q_3+q_4$
λ_3	$P^{(0)}_{3,1}-q_3-q_4$	$P^{(0)}_{3,2}+q_3$	$P^{(0)}_{3,3}+q_3-2q_4$	$P^{(0)}_{3,4}-q_3-q_4$
λ_4	$P^{(0)}_{4,1}+q_3$	$P^{(0)}_{4,2}-q_3-q_4$	$P^{(0)}_{4,3}-q_3+q_4$	$P^{(0)}_{4,4}+q_3$

from which it can be easily seen that q_4 has two significant properties: (1) when $\hat{M}_1 = M_1$ and $\hat{M}_2 = M_2$, q_4 vanishes, which allows one to see that the entire solution reduces to the two-parameter solution in that case; (2) q_4 and q_3 both vanish when $M_2+\hat{M}_1+\hat{M}_2 = 2$, which assures that these function are continuous at $M_2+\hat{M}_1+\hat{M}_2 = 2$. (Continuity is not required, but is desirable on grounds of simplicity.)

To verify that this model has the required properties, one must verify that

$$M_1[y] = M_1, \;\; M_1[y'] = \hat{M}_1, \;\; M_2[x] = M_2, \;\; M_2[x'] = \hat{M}_2, \tag{84}$$

where $M_1[v]$ and $M_2[u]$ were defined by Eqs. (68) and (69), that

$$\sum_{i=1}^{4} p(\lambda_i|u,v) = 1 \tag{85}$$

for all $u \in \{x, x'\}$ and $v \in \{y, y'\}$, that

$$0 \leqslant p(\lambda_i|u,v) \leqslant 1, \tag{86}$$

for all $i \in \{1,2,3,4\}$, $u \in \{x, x'\}$, and $v \in \{y, y'\}$, and finally that

$$S = 2+\min\{\hat{M}_1+\hat{M}_2+\min\{M_1, M_2\},\, 2\}. \tag{87}$$

The verification of these properties, which depends on keeping in mind the restrictions of Eqs. (75) and (77) and the convention $M_1 \geqslant M_2$, is tedious but straightforward.

C. Mutual information of the four-parameter model

Since the four-parameter model reduces to the two-parameter model when $\hat{M}_1 = M_1$ and $\hat{M}_2 = M_2$, it reproduces the two-parameter solution for $M_1 = M_2 = V_T/3$, which gives the quantum violation of the Bell-CHSH inequality (Tsirelson bound) with a very low mutual information, $\approx$0.0463 bits, as per Eq. (62). To show one example of how the mutual information changes when $\hat{M}_1 \neq M_1$ or $\hat{M}_2 \neq M_2$, we show in Fig. 4 a plot of the mutual information of the four-parameter model as a function of z, where $M_1 = M_2 = V_T/3+2z$ and $\hat{M}_1 = \hat{M}_2 = V_T/3-z$, so in all cases $S = 2+V_T$. In this case, the mutual information $I_4(z)$ is given by

$$\begin{aligned} I_4(z) = 1+\frac{3z}{2}+h\left(\frac{2-\sqrt{2}}{4}\right) & \\ +2h\left(\frac{2+\sqrt{2}-6z}{12}\right)+h\left(\frac{2+\sqrt{2}+12z}{12}\right) & \\ -2h\left(\frac{2-3z}{8}\right)-\frac{1}{4}h(1+3z). & \end{aligned} \tag{88}$$

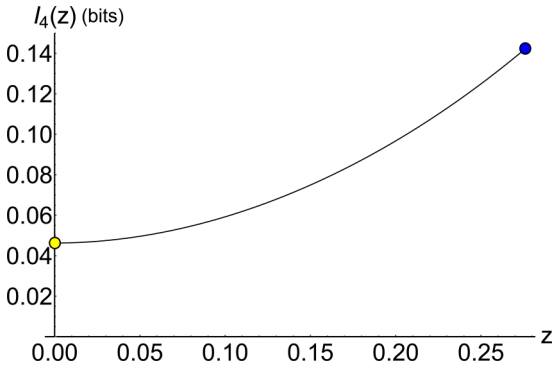

FIG. 4. Plot of mutual information $I_4(z)$, in bits, for the four-parameter model in Table III, for $M_1 \geqslant M_2$ and $M_2 + \hat{M}_1 + \hat{M}_2 \leqslant 2$. $I_4(z)$, given by Eq. (88), is calculated for $M_1 = M_2 = V_T/3 + 2z$, $\hat{M}_1 = \hat{M}_2 = V_T/3 - z$, so in all cases $S = 2 + V_T$. The mutual information $I_4(z)$ is minimized via Eq. (89) when $I_4(0) \approx 0.0463$ bits (light yellow circle) and maximized when $I_4(V_T/3) \approx 0.1423$ bits (dark blue circle).

The mutual information in Eq. (88) is minimized (light yellow circle in Fig. 4) when $z = 0$, yielding

$$I_4(z = 0) = \tilde{I}_G(V_T) \approx 0.0462738 \text{ bits}, \tag{89}$$

which is identical to the value of $\tilde{I}_G(V_T)$ in Eq. (62). $I_4(z)$ grows monotonically with z, to a maximum value of $\approx$0.1423 bits (dark blue circle in Fig. 4) when $z = V_T/3 \approx 0.2761$.

VIII. DISCUSSION

As recognized by Bell himself, the measurement-independence (or freedom-of-choice) assumption is crucial to the derivation of Bell's theorem [3,5]. Relaxing this assumption leads to a potent loophole in the theorem, and opens space for families of locally causal hidden-variable models that could reproduce the quantum predictions for entangled states. As experimental efforts to address the measurement-independence loophole in tests of Bell's inequality continue to improve [11,13–15,24,42,44], it is therefore critical to investigate properties of locally causal models, distinct from quantum mechanics, that could exploit such a loophole to remain viable in the face of various tests.

Building on work in Refs. [30–32], we have constructed a general framework for relaxing the measurement-independence assumption for two-particle tests of Bell's inequality, to accommodate arbitrary amounts of reduced experimental freedom for each observer while satisfying local causality. This framework allows for interpolation between previously studied symmetric models, in which each observer gives up the same amount of freedom [30,31], and one-sided models, in which one observer gives up some freedom while the other maintains perfect freedom [32]. We have derived two new, relaxed Bell-CHSH inequalities for this general framework, which subsume previously studied models as special cases of our more general two- and four-parameter bounds. We show that these bounds are tight by providing local deterministic models which saturate each bound for all regimes of measurement dependence for each observer.

We have also calculated the efficiency of these saturating models for simulating Bell-CHSH violations, as measured by mutual information between the Bell-test detector settings and any hidden variables that affect measurement outcomes. Most interestingly, we find that the two- and four-parameter models in our Tables II and III are very efficient, capable of achieving a given violation of the Bell-CHSH inequality with far less mutual information between the hidden variables and the joint detector settings than is needed by locally causal models that had previously been identified in the literature. We conjecture that our models are optimal in the sense that they achieve (for $M_1 = M_2 = \hat{M}_1 = \hat{M}_2$) the minimum possible mutual information for a given Bell-CHSH violation. Although the interpolating model in Table VI of Appendix A is not optimal compared to Tables II and III, it too requires less mutual information than previously studied models, which it specifically reproduces as special cases.

For each model in this class, we find that only a comparatively small degree of measurement dependence (as measured in bits of mutual information) must be assumed in order to reproduce the predictions from quantum theory, compared to hidden-variable models that exploit other loopholes such as the locality or communication loophole [67] or models that relax determinism [31].

Our framework for considering such models is quite general. For example, while measurement-dependent models allow correlations between the measurement settings and λ, our framework makes no stipulations about where or when in space-time the hidden variable λ is created or becomes relevant; indeed, our formalism remains agnostic about whether λ represents degrees of freedom associated with specific space-time events at all. For example, λ could, in principle, be associated with entire space-time regions or hypersurfaces [68], or with even more fundamental degrees of freedom from which classical space-time (consistent with general relativity) might emerge. Note that the results in this work also apply to stochastic models, and thus are consistent with—but do not require the assumption of—determinism.

We note in particular that relaxing the measurement-independence assumption does not require the additional assumption of "superdeterminism," although the two have at times been conflated in the literature [73,77–84]. For concreteness, we consider the definition of superdeterminism used by 't Hooft [81]: "Superdeterminism may be defined to imply that not only all physical phenomena are declared to be direct consequences of physical laws that do not leave anything anywhere to chance (which we refer to as 'determinism'), but it also emphasizes that the observers themselves behave in accordance with the same laws. ...The fact that an observer cannot reset his or her measuring device without changing physical states in the past is usually thought not to be relevant for our description of physical laws." He further argues, with regard to the correlations between past physical states and present measurement choices [81]: "We claim that not only there are correlations, but the correlations are also extremely strong."

Although the phrase "extremely strong" is only a qualitative statement, one might interpret this claim to mean that in a superdeterministic universe, Alice and Bob would have no freedom whatsoever to choose Bell-test measurement settings,

corresponding to $M = 2$ from Eq. (8) and thus $F = 1 - \frac{M}{2} = 0$ in Eq. (9). Such a maximally deterministic model has been presented by Brans [35]. In contrast to such an "extreme" case of superdeterminism, we note that locally causal models that exploit the measurement-independence loophole, of the sort analyzed here, require quite modest amounts of reduced experimental freedom—as measured by M, M_1, and M_2, or by information-theoretic measures such as mutual information—in order to mimic the predictions from quantum mechanics. (See also Refs. [30–32,64].) In short, relaxation of experimenters' freedom of choice need not be an "all or nothing" assumption. While superdeterminism represents one logical possibility for how the measurement-independence assumption can be relaxed, it is not the only such possibility.

IX. CONCLUSIONS

In this work, we have derived two new, relaxed Bell-CHSH inequalities within a general framework where the assumption of measurement independence can be relaxed to independent degrees for both observers.

In future work, it would be interesting to investigate models of the singlet state compatible with our general bound, generalizing those presented in Refs. [28,30–32], to determine whether there exist locally causal models that can produce the same amount of Bell violation for smaller values of the measurement-dependence parameters M, and/or that would require less mutual information between joint detector settings and hidden variables. It would be of additional interest to further explore whether the results in this work could be generalized to other Bell inequalities beyond Bell-CHSH, for example, those with more than two measurement settings per observer, or those which are not symmetric under correlated flips of the measurement outcomes. The approach we have developed here could also be generalized to locally causal models of correlations among N-particle "GHZ" entangled states (with $N > 2$) [85,86]. Finally, it would be of interest to develop a deeper understanding of this family of locally causal models that relax the measurement-independence assumption in terms of causal space-time structure (e.g., [87]).

ACKNOWLEDGMENTS

The authors would like to thank Anton Zeilinger, Thomas Scheidl, Johannes Handsteiner, Dominik Rauch, Calvin Leung, and David Leon, along with the two anonymous referees, for helpful discussions. A.S.F., A.H.G., D.I.K., and J.G. acknowledge support from NSF INSPIRE Award No. PHY-1541160. Portions of this work were conducted in MIT's Center for Theoretical Physics and supported in part by the US Department of Energy under Contract No. DE-SC0012567. M.J.W.H. acknowledges the support of the Australian Research Council Centre of Excellence CE110001027.

APPENDIX A: INTERPOLATING BETWEEN CHSH MODEL TABLES FROM PREVIOUS WORK

In this Appendix we construct another model that saturates the general two-parameter bound of Eqs. (24) and (25), while at the same time interpolating between the models in Table 1 of Banik *et al.* [32] and Table I of Hall [30] in the physically significant region of parameter space corresponding to $M_1 + M_2 + \min\{M_1, M_2\} \leqslant 2$. At its optimum parameters within this region, the interpolating model requires less mutual information between the hidden variables and detector settings than either the Hall or Banik *et al.* models, although it requires significantly more mutual information than the two-parameter model of Sec. V. In the region for which $M_1 + M_2 + \min\{M_1, M_2\} > 2$, where the Banik *et al.* model does not exist, the interpolating model generalizes the Hall model, reducing to Table II of Hall [30] when $M_1 = M_2$.

TABLE V. Deterministic measurement-outcome functions $A(u, \lambda_i)$ and $B(v, \lambda_i)$ for Alice's and Bob's measurements, given λ_i with $i = 1, \ldots, 5$. The values of the measurement outcomes (c, d, e, f, g) are selected arbitrarily from $\{-1, 1\}$.

λ_i	$A(x, \lambda)$	$A(x', \lambda)$	$B(y, \lambda)$	$B(y', \lambda)$
λ_1	c	c	c	c
λ_2	d	$-d$	d	d
λ_3	e	e	e	$-e$
λ_4	f	$-f$	$-f$	f
λ_5	g	g	g	g

The interpolating model is deterministic and locally causal, with a hidden variable λ that can take on one of 5 discrete values, $\lambda_1, \lambda_2, \ldots, \lambda_5$. For this model the deterministic measurement-outcome functions $A(u, \lambda_i)$, $B(v, \lambda_i)$ for Alice and Bob are of the forms defined in Table V, where the constants c, d, e, f, g may be any values in $\{-1, 1\}$. We divide the square of possible (M_1, M_2) values into six regions, as shown in Fig. 5, and for each region we construct a mapping from the parameters (M_1, M_2) to a set of conditional probabilities, using Tables VI, VII, and VIII, as follows.

Consider first the yellow horizontal hatched region in Fig. 5, which corresponds to $M_1 \geqslant M_2$, $0 \leqslant M_1 \leqslant 2$, $0 \leqslant M_2 \leqslant 2/3$, and $M_1 + 2M_2 \leqslant 2$. For this region, the mapping of the interpolating model will be defined by Table VI. Using Eq. (19) and Tables V and VI, we find that the CHSH parameter S of Eq. (17) takes the form

$$S = 2 + 2p_1 + 4p_2. \tag{A1}$$

Assuming that $p_1 \geqslant p_2$, the degrees of measurement dependence M_1 and M_2, as defined by Eqs. (13) and (14), are found from Table VI to be

$$\begin{aligned} M_1 &= \max\{2p_1, 2p_1\} = 2p_1, \\ M_2 &= \max\{2p_2, 2p_2\} = 2p_2. \end{aligned} \tag{A2}$$

(For Table VI, we also find that $M = \max\{M_1, M_2\} = M_1$.) Thus, Table VI with $p_1 \geqslant p_2$ is a potential model for the region of parameter space for which $M_1 \geqslant M_2$, with $p_1 = M_1/2$ and $p_2 = M_2/2$. To be a viable model, the conditional probabilities that it defines must be non-negative. This will be the case provided that $1 - p_1 - 2p_2 = 1 - \frac{M_1}{2} - M_2 \geqslant 0$, so the region of validity is precisely the yellow horizontal hatched region of Fig. 5. (The total probability for each setting pair must sum to unity, but this can be seen immediately by summing each column of Table VI.)

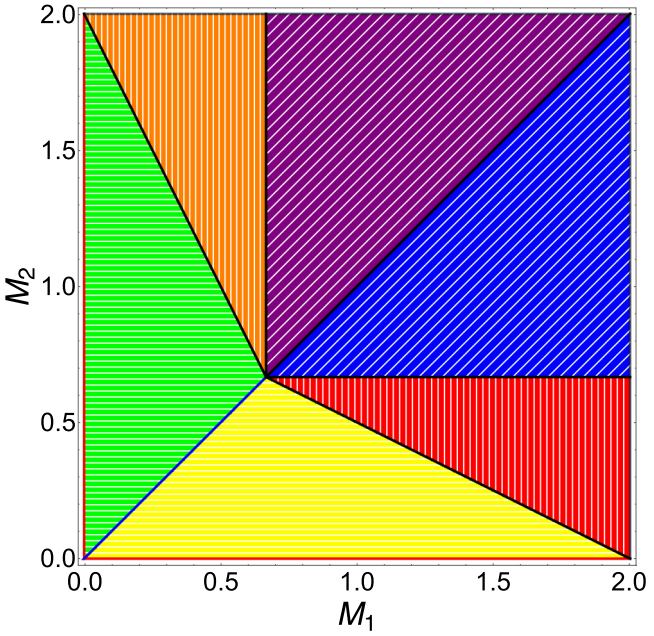

FIG. 5. We construct an "interpolating" model for $p(\lambda_i|u, v)$ for values of (M_1, M_2) in the square of side two. Each point in the square is mapped to a set of conditional probabilities $p(\lambda_i|u, v)$. The yellow horizontal hatched, red vertical hatched, and blue diagonal hatched regions, with $M_1 \geqslant M_2$, are mapped according to the entries in Tables VI–VIII. Tables corresponding to the green horizontal hatched, orange vertical hatched, and purple diagonal hatched regions, with $M_2 \geqslant M_1$, may be constructed by swapping Alice's and Bob's detector-setting labels, $x \leftrightarrow y, x' \leftrightarrow y'$, as well as the labels $1 \leftrightarrow 2$. The model saturates the general two-parameter bound, providing an additional proof that the bound is tight.

Given that $p_1 = M_1/2$ and $p_2 = M_2/2$, Eq. (A1) implies that

$$S = 2 + M_1 + M_2 + \min\{M_1, M_2\}, \tag{A3}$$

saturating the upper bound derived in Eq. (24) for the case in which $M_1 + M_2 + \min\{M_1, M_2\} \leqslant 2$.

We proceed similarly for the red vertical hatched and blue diagonal hatched regions of Fig. 5, which both satisfy $M_1 \geqslant M_2$ and $M_1 + 2M_2 \geqslant 2$. The red vertical hatched region corresponds to $2/3 \leqslant M_1 \leqslant 2$ and $0 \leqslant M_2 \leqslant 2/3$, and is described in the interpolating model by Table VII. Assuming that $p_1 \leqslant 1$, $p_2 \leqslant 1/3$, and $p_1 + 2p_2 \geqslant 1$, we find from Table VII

TABLE VI. Conditional probabilities $p(\lambda_i|u, v)$ for the value of the hidden variable λ to be λ_i, for $M_1 + M_2 + \min\{M_1, M_2\} \leqslant 2$, $0 \leqslant M_1 \leqslant 2$, $0 \leqslant M_2 \leqslant 2/3$, and $M_1 \geqslant M_2$ (Fig. 5, yellow horizontal hatched region).

λ_i	$p(\lambda\|x, y)$	$p(\lambda\|x, y')$	$p(\lambda\|x', y)$	$p(\lambda\|x', y')$
λ_1	p_2	p_2	p_2	0
λ_2	p_2	p_2	0	p_2
λ_3	p_2	0	p_1	p_1
λ_4	0	p_2	p_2	p_2
λ_5	$1 - 3p_2$	$1 - 3p_2$	$1 - p_1 - 2p_2$	$1 - p_1 - 2p_2$

TABLE VII. Conditional probabilities $p(\lambda_i|u, v)$ for the case $M_1 + M_2 + \min\{M_1, M_2\} \geqslant 2$, $2/3 \leqslant M_1 \leqslant 2$, $0 \leqslant M_2 \leqslant 2/3$, and $M_1 \geqslant M_2$ (Fig. 5, red vertical hatched region).

λ_i	$p(\lambda\|x, y)$	$p(\lambda\|x, y')$	$p(\lambda\|x', y)$	$p(\lambda\|x', y')$
λ_1	p_2	p_2	$\frac{1}{2}(1 - p_1)$	0
λ_2	p_2	p_2	0	$\frac{1}{2}(1 - p_1)$
λ_3	p_2	0	$\frac{1}{2}(1 - p_1)$	$\frac{1}{2}(1 - p_1)$
λ_4	0	p_2	p_1	p_1
λ_5	$1 - 3p_2$	$1 - 3p_2$	0	0

that

$$\begin{aligned} M_1 &= \max\{2p_1, 1 + p_1 - 2p_2\} = 2p_1, \\ M_2 &= \max\{2p_2, 1 - p_1\} = 2p_2. \end{aligned} \tag{A4}$$

(We again find that $M = M_1$.) In this case no additional constraints are imposed by non-negativity, but the constraints that we imposed to evaluate M_1 and M_2 are precisely the conditions that delineate the red vertical hatched region of Fig. 5.

The blue diagonal hatched region corresponds to $2/3 \leqslant M_1 \leqslant 2$, $2/3 \leqslant M_2 \leqslant 2$, again with $M_1 \geqslant M_2$, and is described in the interpolating model by Table VIII, with

$$\begin{aligned} p_1 &= \frac{2 - M_2}{4} + \frac{M_1 - M_2}{12}, \\ p_2 &= \frac{M_1 - M_2}{6}, \\ p_3 &= \begin{cases} 0, & \text{if } M_1 \leqslant 4M_2 - 2, \\ \frac{1}{8}(M_1 - 4M_2 + 2), & \text{otherwise.} \end{cases} \end{aligned} \tag{A5}$$

When $M_1 = M_2$, p_2 and p_3 vanish, and p_1 becomes equal to the value of p in Table II of Hall [30], making our Table VIII an exact match for Table II of Hall. Using Table VIII and Eqs. (A5), one can verify that

$$\begin{aligned} M_1[y] &= M_1, \\ M_1[y'] &= \begin{cases} 2M_2 - M_1, & \text{if } M_1 \leqslant 4M_2 - 2, \\ 2 - 2M_2, & \text{otherwise,} \end{cases} \\ M_2[x] &= M_2, \\ M_2[x'] &= M_2, \end{aligned} \tag{A6}$$

where we are using the definitions in Eqs. (68) and (69). For the parameter range of the blue diagonal hatched region, it is easily seen that $\max(M_1[y], M_1[y']) = M_1$, as desired. One can also verify that the probabilities in each column of Table VIII sum to 1, and that all the entries of the table are non-negative for (M_1, M_2) in the blue diagonal hatched region of Fig. 5. Thus, in the blue diagonal hatched region Table VIII defines a consistent set of conditional probabilities that match the Hall model when $M_1 = M_2$. (We again find that $M = M_1$.)

Upon using Tables VII and VIII together with the measurement outcomes in Table V, we find $S = 4$ for both the red vertical hatched and blue diagonal hatched regions, saturating the upper bound in Eqs. (24) and (25). To our knowledge, the

TABLE VIII. Conditional probabilities $p(\lambda_i|u,v)$ for the case $M_1+M_2+\min\{M_1,M_2\}\geqslant 2$, $2/3\leqslant M_1, M_2\leqslant 2$, and $M_1\geqslant M_2$ (Fig. 5, blue diagonal hatched region).

λ_i	$p(\lambda\|x,y)$	$p(\lambda\|x,y')$	$p(\lambda\|x',y)$	$p(\lambda\|x',y')$
λ_1	p_1-2p_2	$\frac{1-p_1}{2}-2p_2+p_3$	$\frac{1-p_1}{2}+p_2-p_3$	0
λ_2	$\frac{1-p_1}{2}+4p_2-p_3$	p_1+p_2	0	$\frac{1-p_1}{2}+p_2-p_3$
λ_3	$\frac{1-p_1}{2}-2p_2+p_3$	0	$p_1-2p_2+2p_3$	$\frac{1-p_1}{2}-2p_2+3p_3$
λ_4	0	$\frac{1-p_1}{2}+p_2-p_3$	$\frac{1-p_1}{2}+p_2-p_3$	$p_1+p_2-2p_3$
λ_5	0	0	0	0

model represented by Tables V–VIII has not been described previously in the literature.

Thus the interpolating model, as defined by Tables V–VIII, saturates the two-parameter general bound for all values $M_1\geqslant M_2$. By symmetry, one can complete the definition of the interpolating model by constructing equivalent tables for $M_2\geqslant M_1$, by switching settings labels $x\leftrightarrow y$, $x'\leftrightarrow y'$ and subscripts $1\leftrightarrow 2$. Since the interpolating model saturates the two-parameter bound of Eq. (25), it provides an additional proof that Eq. (25) is a tight upper bound on S for hidden-variable models that obey local causality but do not obey measurement independence.

To show how the interpolating model is related to the Hall model of Table I of Ref. [30] and the Banik *et al.* model of Table 1 of Ref. [32], we introduce a notation that uses subscripts to show explicitly the dependence of the conditional probabilities $p(\lambda_i|u,v)$ on the parameters p_1 and p_2. In particular, we will denote the entries of Table VI by

$$p^{VI}_{p_1,p_2}(\lambda_i|u,v), \tag{A7}$$

and the entries of the Hall model by

$$p^{H}_{p}(\lambda_i|u,v). \tag{A8}$$

Table I of Ref. [32] has only two rows, but they can be identified with rows 3 and 5 of the other models, with the remaining rows set to zero. Thus, the conditional probabilities of the Banik *et al.* model can be denoted by

$$p^{B}_{p}(\lambda_i|u,v). \tag{A9}$$

It is then easily seen that for $M_1\geqslant M_2$ and $M_1+2M_2\leqslant 2$, when Table VI applies, the interpolating model exactly matches the two previous models in the appropriate limits:

$$p^{VI}_{p,p}(\lambda_i|u,v)=p^{H}_{p}(\lambda_i|u,v), \tag{A10}$$

$$p^{VI}_{p,0}(\lambda_i|u,v)=p^{B}_{p}(\lambda_i|u,v). \tag{A11}$$

Furthermore, for general values it is simply a linear interpolation:

$$p^{VI}_{p_1,p_2}(\lambda_i|u,v)=wp^{H}_{p_1}(\lambda_i|u,v)+(1-w)p^{B}_{p_1}(\lambda_i|u,v), \tag{A12}$$

where $w=p_2/p_1$.

APPENDIX B: MUTUAL INFORMATION FOR THE INTERPOLATING MODEL

Just as in Sec. VI, we can compute the mutual information between the hidden variable λ and the detector settings for the interpolating model, using Eqs. (50)–(53) and the measurement outcomes from Table V. Here we consider the case $M_1\geqslant M_2$ and the range $M_1+2M_2\leqslant 2$ with violations $V\in[0,2]$, so Table VI applies.

Using Table VI and Eq. (51), and recalling that $p_1=M_1/2$, $p_2=M_2/2$ in this model, we find that the mutual information for the interpolating model is given by

$$\begin{aligned}I_I(M_1,M_2)&=\frac{1}{4}\sum_{i,u,v}p(\lambda_i|u,v)\log_2 p(\lambda_i|u,v)\\&\quad-\sum_i p(\lambda_i)\log_2 p(\lambda_i)\\&=\frac{1}{4}\left\{2h\left(\frac{2-3M_2}{2}\right)+2h\left(\frac{2-M_1-2M_2}{2}\right)\right.\\&\quad-4h\left(\frac{2M_1+M_2}{8}\right)-4h\left(\frac{4-M_1-5M_2}{4}\right)\\&\quad\left.+2h\left(\frac{M_1}{2}\right)+h\left(\frac{M_2}{2}\right)+\frac{9M_2}{2}\log_2\frac{4}{3}\right\}.\end{aligned} \tag{B1}$$

Equation (B1) is plotted in Fig. 6.

Using the relation $M_1=V-2M_2$ for models that saturate the general two-parameter bound, we can also express I_I in

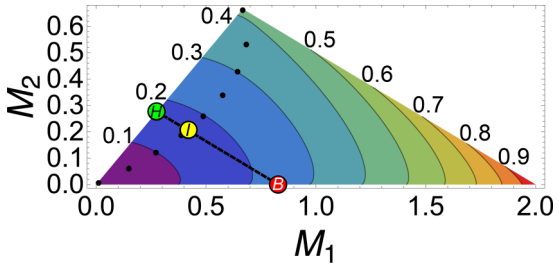

FIG. 6. "Freedom square" plot labeled by contours of mutual information $I_I(M_1,M_2)$ for the interpolating model, in bits, from Eq. (B1) derived from Table VI. The Hall and Banik *et al.* subcases are denoted by light green (H) and dark red (B) circles, respectively, with the light yellow circle (I) showing where mutual information is minimized for the interpolating model. The dashed line is the slice satisfying $V(M_1,M_2)=V_T$, connecting solutions for the Hall model $(M_1,M_2)=(V_T/3,V_T/3)$, and the Banik model $(M_1,M_2)=(V_T,0)$, with minimum mutual information $I_I(\bar{M}_1,\bar{M}_2)\approx 0.1616$ at $(\bar{M}_1,\bar{M}_2)\approx(0.4158,0.2063)$. See Fig. 7 (top). The black dots, plus the light yellow circle (I), trace the curve that minimizes the mutual information for each value of Bell violation $V\in[0,2]$. See Fig. 7 (bottom).

terms of M_2 and the amount of violation V:

$$\tilde{I}_I(V, M_2) \equiv I_I(V - 2M_2, M_2) = \frac{1}{4}\left\{2h\left(\frac{V-2M_2}{2}\right) + h\left(\frac{M_2}{2}\right) + \frac{9M_2}{2}\log_2\frac{4}{3} - 4h\left(\frac{2V-3M_2}{8}\right) - 4h\left(\frac{4-V-3M_2}{4}\right) + 2h\left(\frac{2-3M_2}{2}\right) + 2h\left(\frac{2-V}{2}\right)\right\}, \quad \text{(B2)}$$

with M_2 restricted to the range $0 \leqslant M_2 \leqslant V/2 \leqslant 2$. We denote the minimum of $\tilde{I}_I(V, M_2)$, minimized over M_2, by $\tilde{I}_I(V)$.

The mutual information requirements of the Hall model of Ref. [30] and the Banik *et al.* model of Ref. [32] were discussed in Sec. VI. The mutual information required for each model, to achieve a specified Bell-CHSH inequality violation V, was specified in Eq. (59) for $I_H(V)$ and Eq. (60) for $I_B(V)$. These functions were plotted in Fig. 3 in comparison with $\tilde{I}_G(V)$, the minimum mutual information for the two-parameter model of Sec. V. In the top panel of Fig. 7, the same two functions are shown in comparison with $\tilde{I}_I(V)$, the minimum mutual information for the interpolating model. $\tilde{I}_I(V)$ is less than either of these two comparison models, but it is nonetheless significantly larger that the mutual information required by the two-parameter model of Sec. V. For the maximum quantum violation V_T, the Banik *et al.* model requires 0.247 bits of mutual information, the Hall model requires 0.172 bits, and the interpolating model requires 0.162 bits. The two-parameter model of Sec. V requires only 0.0462 bits, as shown in Eq. (62).

The lower panel of Fig. 7 shows the mutual information of the interpolating model, $\tilde{I}_I(V_T, M_2)$, for the maximum quantum violation V_T, shown in bits as a function of M_2. The minimum occurs at $M_1 \approx 0.416$ and $M_2 \approx 0.206$ [yellow circle (I)].

Overall, while the interpolating model requires less mutual information between the settings and hidden variables to mimic the quantum predictions for violations of the Bell-CHSH inequality than previously studied locally causal models, it is significantly less efficient than the two-parameter model of Sec. V.

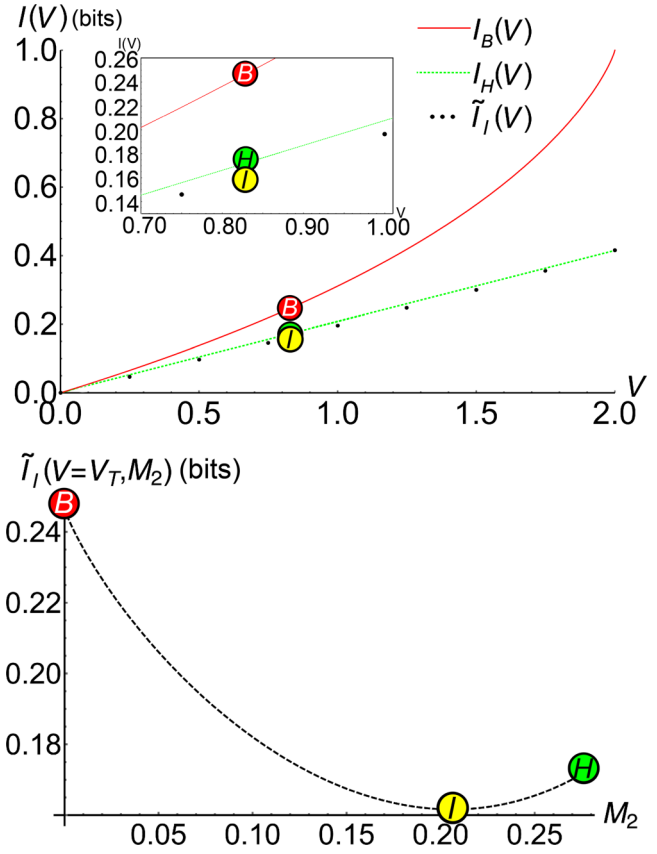

FIG. 7. These plots use the interpolating model with $V(M_1, M_2) = M_1 + 2M_2 \leqslant 2$, $M_1 \geqslant M_2$. As in Fig. 6, large colored circles marked with B, H, or I denote $V(M_1, M_2) = V_T$ for the Banik, Hall, and interpolating models, respectively. The interpolating model, which for these parameters is defined by Table VI, requires less mutual information (light yellow circle) to produce a given Bell violation than the previously studied Hall and Banik *et al.* subcases, denoted by light green and dark red circles, respectively. Top: Mutual information for the Hall model (dotted green curve), the Banik *et al.* model (solid red curve), and the minimum of the interpolating model $\tilde{I}_I(V) \equiv \min_{M_2} \tilde{I}_I(V, M_2)$ (black dots, as in Fig. 6), in bits, plotted as a function of CHSH violation $V \in [0, 2]$ (see inset plot). The Hall model always requires less mutual information than the Banik model to produce a given Bell violation, while the minimum of the interpolating model requires even less mutual information than the Hall or Banik models. Bottom: Mutual information $\tilde{I}_I(V_T, M_2)$ required to reach the Tsirelson bound $V(M_1, M_2) = V_T$ (e.g., dashed black line in Fig. 6), plotted in bits as a function of $M_2 \in [0, V_T/3]$.

APPENDIX C: STEPS IN PROOF OF THE FOUR-PARAMETER RELAXED BELL-CHSH INEQUALITY

We wish to prove that the inequality

$$T_1 \leqslant 2 + M_1[y'] \quad \text{(C1)}$$

from Eq. (70) holds.

Starting with Eq. (26), we replace Eq. (27) with

$$S = \left| \int d\lambda \{ p(\lambda|x, y')[A(x, \lambda)B(y', \lambda) + A(x, \lambda)B(y, \lambda)] - p(\lambda|x', y')[A(x', \lambda)B(y', \lambda) - A(x', \lambda)B(y, \lambda)] + A(x, \lambda)B(y, \lambda)[p(\lambda|x, y) - p(\lambda|x, y')] + A(x', \lambda)B(y, \lambda)[p(\lambda|x', y) - p(\lambda|x', y')] \} \right|. \quad \text{(C2)}$$

Then

$$S \leqslant \tilde{T}_1 + \tilde{T}_2 + \tilde{T}_3, \quad \text{(C3)}$$

where

$$\tilde{T}_1 = \int d\lambda |p(\lambda|x, y')[A(x, \lambda)B(y', \lambda) + A(x, \lambda)B(y, \lambda)] - p(\lambda|x', y')[A(x', \lambda)B(y', \lambda) - A(x', \lambda)B(y, \lambda)]|, \quad \text{(C4)}$$

$$\tilde{T}_2 = \int d\lambda |A(x, \lambda)B(y, \lambda)[p(\lambda|x, y) - p(\lambda|x, y')]|, \quad \text{(C5)}$$

and

$$\tilde{T}_3 = \int d\lambda |A(x',\lambda)B(y,\lambda)[p(\lambda|x',y) - p(\lambda|x',y')]|. \tag{C6}$$

Clearly

$$\tilde{T}_2 + \tilde{T}_3 = M_2 + \hat{M}_2, \tag{C7}$$

and $\tilde{T}_1$ can be rewritten as

$$\begin{aligned}
\tilde{T}_1 &= \int d\lambda |B(y,\lambda)[A(x,\lambda)p(\lambda|x,y') + A(x',\lambda)p(\lambda|x',y')] \\
&\quad + B(y',\lambda)[A(x,\lambda)p(\lambda|x,y') - A(x',\lambda)p(\lambda|x',y')]| \\
&\leqslant \int d\lambda \left\{ \left| B(y,\lambda)A(x,\lambda)\left[p(\lambda|x,y') \right.\right.\right. \\
&\quad \left.\left.\left. + \frac{A(x',\lambda)}{A(x,\lambda)} p(\lambda|x',y') \right] \right| + \left| B(y',\lambda)A(x,\lambda) \right. \\
&\quad \left. \times \left[p(\lambda|x,y') - \frac{A(x',\lambda)}{A(x,\lambda)} p(\lambda|x',y') \right] \right| \Bigg\} \\
&\leqslant \int d\lambda \left\{ \left| p(\lambda|x,y') + \frac{A(x',\lambda)}{A(x,\lambda)} p(\lambda|x',y') \right| \right. \\
&\quad \left. + \left| p(\lambda|x,y') - \frac{A(x',\lambda)}{A(x,\lambda)} p(\lambda|x',y') \right| \right\} \\
&\leqslant 2 + M_1[y'],
\end{aligned} \tag{C8}$$

as we had claimed.

APPENDIX D: CONSTRUCTION OF THE FOUR-PARAMETER MODEL

The two-parameter model of Sec. V was found by trial and error, but attempts at finding a four-parameter model using trial and error did not succeed. But there is a more systematic way, based on examining the proof of the bound in Sec. VII, identifying the conditions that are needed to saturate it. We describe this systematic approach in some detail in this appendix, as we believe the basic ideas are of general value to the construction of saturating models.

Without loss of generality we can seek a solution with $M_1 \geqslant M_2$, because the opposite case can be treated by interchanging the labels 1 and 2, which is equivalent to interchanging (x, x') with (y, y'). Similarly, we can without loss of generality seek a solution with $M_1[y] \geqslant M_1[y']$, because the opposite case can be treated by interchanging the labels y and y'. Thus, our solution will have $M_1 = M_1[y]$ and $\hat{M}_1 = M_1[y']$. Finally, we can without loss of generality seek a solution with $M_2[x] \geqslant M_2[x']$, so the solution will have $M_2 = M_2[x]$ and $\hat{M}_2 = M_2[x']$.

The proof involved showing two bounds on T_1: $T_1 \leqslant 2 + M_1[y]$ and $T_1 \leqslant 2 + M_1[y']$. For the conventions adopted in the previous paragraph, it is the second of these bounds that is the more stringent, so it is the second that must be saturated. This means that we must examine the bound that was demonstrated in Appendix C, Eqs. (C2)–(C8). We initially restrict ourselves to the case $M_2 + \hat{M}_1 + \hat{M}_2 \leqslant 2$, since it is only in this case that the bound shown in Eq. (72) is saturated.

Starting with Eq. (C2) for S, we recognize that the integral over λ reduces for our model to the sum over the four values of λ: $\lambda_1 \ldots \lambda_4$, as listed in Table I. The bound is established by rewriting the integrand as the sum of judiciously chosen pieces, and then bounding the absolute value of the integral by the sum of the integrals of the absolute values of the pieces. The bound will therefore be equal to S if each of the pieces is positive, so the absolute value signs become irrelevant. (The bound would also be saturated if all the pieces were negative, but we did not pursue this option.) Thus, we will examine each piece, and insist that it be positive.

We start with the third line of Eq. (C2), which are the terms that are bounded by $\tilde{T}_2$, as shown in Eq. (C5). The signs are determined by the product $A(x|\lambda_i)B(y|\lambda_i)$, which according to Table I is equal to 1 for $i = 1, 2, 3$, and -1 for $i = 4$. Thus, if all terms are to be positive, we need

$$p(\lambda_i|x,y) - p(\lambda_i|x,y') \begin{cases} \geqslant 0, & \text{for } i = 1,2,3, \\ \leqslant 0, & \text{for } i = 4. \end{cases} \tag{D1}$$

Next, we examine the fourth line of Eq. (C2), which shows the terms that are bounded by $\tilde{T}_3$, as shown in Eq. (C6). In this case the signs are controlled by the product $A(x'|\lambda_i)B(y|\lambda_i)$, which according to Table I is equal to 1 for $i = 1, 3, 4$, and -1 for $i = 2$. Thus, we require

$$p(\lambda_i|x',y) - p(\lambda_i|x',y') \begin{cases} \geqslant 0, & \text{for } i = 1,3,4, \\ \leqslant 0, & \text{for } i = 2. \end{cases} \tag{D2}$$

Finally, we examine the first two lines of Eq. (C2), which are the terms that are bounded by $\tilde{T}_1$. Arranging the terms as in Eq. (C8), the relevant signs are determined by $B(y|\lambda_i)A(x|\lambda_i)$, which is 1 for $i = 1, 2, 3$, and -1 for $i = 4$; by $A(x'|\lambda_i)/A(x|\lambda_i)$, which is 1 for $i = 1, 3$, and -1 for $i = 2, 4$; and by $B(y'|\lambda_i)A(x|\lambda_i)$, which is 1 for $i = 1, 2, 4$, and -1 for $i = 3$. Using these signs, one can write the sum as

$$\begin{aligned}
\tilde{T}_1 \leqslant |\{ & [p(\lambda_1|x,y') + p(\lambda_1|x',y')] \\
& + [p(\lambda_1|x,y') - p(\lambda_1|x',y')] \\
& + [p(\lambda_2|x,y') + p(\lambda_2|x',y')] \\
& + [p(\lambda_2|x,y') - p(\lambda_2|x',y')] \\
& + [p(\lambda_3|x,y') + p(\lambda_3|x',y')] \\
& + [p(\lambda_3|x',y') - p(\lambda_3|x,y')] \\
& + [p(\lambda_4|x,y') + p(\lambda_4|x',y')] \\
& + [p(\lambda_4|x',y') - p(\lambda_4|x,y')]\}|.
\end{aligned} \tag{D3}$$

Thus, the terms will all be positive provided that we insist that

$$p(\lambda_i|x,y') - p(\lambda_i|x',y') \begin{cases} \geqslant 0, & \text{for } i = 1,2, \\ \leqslant 0, & \text{for } i = 3,4. \end{cases} \tag{D4}$$

To enforce these conditions, we parametrize the conditional probability table as in Table IX, which is designed so that the inequalities of Eqs. (D1), (D2), and (D4) are all enforced by the conditions $f_i \geqslant 0$ for all i.

Since we would like our four-parameter model to reduce to the two-parameter model of Sec. V when $\hat{M}_1 = M_1$ and $\hat{M}_2 = M_2$, it is useful to list the values of the f's for the two-

TABLE IX. Parametrization of the conditional probabilities $p(\lambda_i|u,v)$, with the property that the inequalities described by Eqs. (D1), (D2), and (D4) are all enforced by the conditions $f_i \geqslant 0$ for all i.

λ_i	$p(\lambda\|x,y)$	$p(\lambda\|x,y')$	$p(\lambda\|x',y)$	$p(\lambda\|x',y')$
λ_1	$f_1+f_5+f_6$	f_1+f_5	f_1+f_7	f_1
λ_2	$f_2+f_8+f_9+f_{10}$	$f_2+f_8+f_9$	f_2	f_2+f_8
λ_3	f_3+f_{13}	f_3	$f_3+f_{11}+f_{12}$	f_3+f_{11}
λ_4	f_4	f_4+f_{14}	$f_4+f_{14}+f_{15}+f_{16}$	$f_4+f_{14}+f_{15}$

parameter model (for $M_2+\hat{M}_1+\hat{M}_2 \leqslant 2$):

$$\begin{aligned} f_1 &= (2-M_1-2M_2)/8, \quad f_2 = (2-M_1-2M_2)/8, \\ f_3 &= (2-M_1-2M_2)/8, \quad f_4 = (2-M_1-2M_2)/8, \\ f_5 &= (M_1+M_2)/4, \quad f_6 = 0, \quad f_7 = M_2/2, \\ f_8 &= M_2/2, \quad f_9 = (M_1-M_2)/4, \quad f_{10} = 0, \\ f_{11} &= (M_1+M_2)/4, \quad f_{12} = 0, \quad f_{13} = M_2/2, \\ f_{14} &= M_2/2, \quad f_{15} = (M_1-M_2)/4, \quad f_{16} = 0. \end{aligned} \tag{D5}$$

The requirement that the model saturate the bound that $S \leqslant 2+M_2+\hat{M}_1+\hat{M}_2$ can be expressed using Eq. (26) for S, with Table I. The result can be written most simply if one also uses the normalization of probabilities, which gives

$$\begin{aligned} S &= 4-2[p(\lambda_1|x',y')+p(\lambda_2|x',y) \\ &\quad +p(\lambda_3|x,y')+p(\lambda_4|x,y)] \\ &= 4-2(f_1+f_2+f_3+f_4), \end{aligned} \tag{D6}$$

so saturation implies that

$$f_1+f_2+f_3+f_4 = 1-\tfrac{1}{2}(M_2+\hat{M}_1+\hat{M}_2). \tag{D7}$$

Using this equation, the normalization equations are found to be equivalent to

$$f_6+f_{10}+f_{13} = f_{14}, \tag{D8}$$

$$f_7+f_{12}+f_{16} = f_8, \tag{D9}$$

$$f_5+f_8+f_9+f_{14} = \tfrac{1}{2}(M_2+\hat{M}_1+\hat{M}_2), \tag{D10}$$

$$f_8+f_{11}+f_{14}+f_{15} = \tfrac{1}{2}(M_2+\hat{M}_1+\hat{M}_2). \tag{D11}$$

We next calculate

$$\begin{aligned} M_1 = M_1[y] &= f_8+f_9+f_{10}+f_{14}+f_{15}+f_{16} \\ &\quad +|f_{11}+f_{12}-f_{13}|+|f_5+f_6-f_7|, \end{aligned} \tag{D12}$$

$$M_2 = M_2[x] = f_6+f_{10}+f_{13}+f_{14}, \tag{D13}$$

$$\hat{M}_1 = M_1[y'] = f_5+f_9+f_{11}+f_{15}, \tag{D14}$$

$$\hat{M}_2 = M_2[x'] = f_7+f_8+f_{12}+f_{16}. \tag{D15}$$

By combining Eq. (D8) with Eq. (D13), and Eq. (D9) with Eq. (D15), one has immediately

$$f_{14} = \tfrac{1}{2}M_2, \tag{D16}$$

$$f_8 = \tfrac{1}{2}\hat{M}_2, \tag{D17}$$

and then Eqs. (D8)–(D11) become

$$f_6+f_{10}+f_{13} = \tfrac{1}{2}M_2, \tag{D18}$$

$$f_7+f_{12}+f_{16} = \tfrac{1}{2}\hat{M}_2, \tag{D19}$$

$$f_5+f_9 = \tfrac{1}{2}\hat{M}_1, \tag{D20}$$

$$f_{11}+f_{15} = \tfrac{1}{2}\hat{M}_1. \tag{D21}$$

To make use of Eq. (D12) for M_1, one needs to evaluate the two expressions inside absolute value signs. From Eq. (D5), we see that each expression is non-negative in the two-parameter model. Since we would like the four-parameter model to reduce to the two-parameter model, we will assume that these expressions are non-negative here:

$$f_{11}+f_{12}-f_{13} \geqslant 0, \tag{D22}$$

$$f_5+f_6-f_7 \geqslant 0, \tag{D23}$$

in which case Eq. (D12) simplifies to

$$f_7+f_{13} = \tfrac{1}{2}[M_2+\hat{M}_2-(M_1-\hat{M}_1)]. \tag{D24}$$

From Eqs. (D5), we see that for the two-parameter solution, $f_6 = f_{10} = f_{12} = f_{16} = 0$. At this point we will assume that the four-parameter solution we seek maintains the property that

$$f_{10} = f_{16} = 0, \tag{D25}$$

although we will see that it will not be possible to also require f_6 and f_{12} to vanish. We will find such a solution, which is our goal, and we make no claims that we will find all solutions. Then Eqs. (D18) and (D19) can be solved for f_{13} and f_7, which allows us to rewrite Eqs. (D22)–(D24) as

$$f_{11} \geqslant \tfrac{1}{2}(M_2-M_1+\hat{M}_1), \tag{D26}$$

$$f_5 \geqslant \tfrac{1}{2}(\hat{M}_2-M_1+\hat{M}_1), \tag{D27}$$

$$f_6+f_{12} = \tfrac{1}{2}(M_1-\hat{M}_1), \tag{D28}$$

and the constraints $f_{13} \geqslant 0$ and $f_7 \geqslant 0$ become

$$f_6 \leqslant \tfrac{1}{2}M_2, \tag{D29}$$

$$f_{12} \leqslant \tfrac{1}{2}\hat{M}_2. \tag{D30}$$

Consider first the values of f_6 and f_{12}. Equations (D28)–(D30) specify the sum of these two quantities, and upper limits for each. The limit for f_6 is greater than or equal to the limit for f_{12}. The sum may or may not be smaller than the individual limits, but Eq. (77) guarantees that the sum is always less than or equal to the sum of the limits, so the equations can always be satisfied. A simple solution is to

assign the full sum to f_6, if the sum is less than the upper limit, and otherwise to set f_6 equal to its upper limit, and assign the balance of the sum to f_{12}:

$$f_6 = \tfrac{1}{2}\min(M_1\text{-}\hat{M}_1, M_2), \tag{D31}$$

$$f_{12} = \tfrac{1}{2}[M_1 - \hat{M}_1 - \min(M_1\text{-}\hat{M}_1, M_2)]. \tag{D32}$$

Given that we have chosen to set $f_{10} = f_{16} = 0$, Eqs. (D18) and (D19) can now be used to show that

$$f_7 = \tfrac{1}{2}[\hat{M}_1 + \hat{M}_2 - M_1 + \min(M_1 - \hat{M}_1, M_2)], \tag{D33}$$

$$f_{13} = \tfrac{1}{2}[M_2 - \min(M_1 - \hat{M}_1, M_2)]. \tag{D34}$$

Now consider the values of f_5 and f_9, where the sum is given by Eq. (D20) and a lower bound on f_5 is given by Eq. (D27). Both f_5 and f_9 must be non-negative, which may or may not be a more stringent bound for f_5 than Eq. (D27), depending on parameters. In addition, Eq. (D5) shows the values we would like these functions to have when $\hat{M}_1 = M_1$ and $\hat{M}_2 = M_2$. A reasonably simple solution satisfying all these properties is given by

$$f_5 = \tfrac{1}{4}[\hat{M}_1 + M_2 - \min(M_1 - \hat{M}_1, M_2)], \tag{D35}$$

$$f_9 = \tfrac{1}{4}[\hat{M}_1 - M_2 + \min(M_1 - \hat{M}_1, M_2)]. \tag{D36}$$

The discussion of f_{11} and f_{15} is almost identical to that of f_5 and f_9, except that the first terms on the right-hand sides of Eqs. (D26) and (D27) are different. But the same solution satisfies all the conditions:

$$f_{11} = \tfrac{1}{4}[\hat{M}_1 + M_2 - \min(M_1 - \hat{M}_1, M_2)], \tag{D37}$$

$$f_{15} = \tfrac{1}{4}[\hat{M}_1 - M_2 + \min(M_1 - \hat{M}_1, M_2)]. \tag{D38}$$

Finally, we need to choose values of f_1–f_4 consistent with the sum in Eq. (D7). Following the two-parameter expressions in Eq. (D5), we choose them to be equal, so

$$f_1 = f_2 = f_3 = f_4 = \tfrac{1}{8}(2 - M_2 - \hat{M}_1 - \hat{M}_2). \tag{D39}$$

All of the f's have now been specified, and putting it all together leads to Table III.

To extend the model into the region $M_2 + \hat{M}_1 + \hat{M}_2 > 2$, as is shown in Table IV, there is again a systematic method, but again it involves some arbitrary choices, so the answer is not unique.

Suppose that we are given an arbitrary allowed set of parameter values, $(M_1, M_2, \hat{M}_1, \hat{M}_2)$, consistent with Eqs. (75) and (77), and the labeling convention that $M_1 \geqslant M_2$. Our goal is to construct a table of conditional probabilities consistent with these parameters.

If $M_2 + \hat{M}_1 + \hat{M}_2 \leqslant 2$, then we of course just use the solution already constructed. But if the same table is used when $M_2 + \hat{M}_1 + \hat{M}_2 > 2$, one sees immediately that the terms on the diagonal running from lower left to upper right (hereafter, the main diagonal) all become negative. Saturation for $M_2 + \hat{M}_1 + \hat{M}_2 > 2$ implies $S = 4$, which with Eq. (D6) implies that the sum of the main diagonal terms must vanish, which in turn implies that each term on the main diagonal must vanish, since they cannot be negative. It is thus clear that

TABLE X. Definition of the matrix $G_{i,j}$, where the matrix of conditional probabilities for the four-parameter model, when $M_2 + \hat{M}_1 + \hat{M}_2 > 2$, is written as $P_{i,j} = P^{(0)}_{i,j} + G_{i,j}$, where $P^{(0)}_{i,j}$ is the matrix in Table III.

λ_i	$p(\lambda\|x, y)$	$p(\lambda\|x, y')$	$p(\lambda\|x', y)$	$p(\lambda\|x', y')$
λ_1	$g_1 + g_2$	$-g_3 - h$	$-g_5 - h$	$2h$
λ_2	$-g_1 - h$	$g_3 + g_4$	$2h$	$-g_7 - h$
λ_3	$-g_2 - h$	$2h$	$g_5 + g_6$	$-g_8 - h$
λ_4	$2h$	$-g_4 - h$	$-g_6 - h$	$g_7 + g_8$

for $M_2 + \hat{M}_1 + \hat{M}_2 > 2$, the terms on the main diagonal of Table III must be adjusted by adding a quantity $2h$, given by

$$h = \tfrac{1}{2}q_3 = \tfrac{1}{16}(M_2 + \hat{M}_1 + \hat{M}_2 - 2), \tag{D40}$$

where q_3 is defined in Eq. (80). We initially allow arbitrary variation of the other entries, requiring however that the sum for each row remain equal to 1. Such an arbitrary variation can be parametrized by the matrix $G_{i,j}$ shown in Table X, where the full conditional probabilities for $M_2 + \hat{M}_1 + \hat{M}_2 > 2$ will be given by

$$P_{i,j} = P^{(0)}_{i,j} + G_{i,j}, \tag{D41}$$

where $P^{(0)}_{i,j}$ is the matrix defined by Table III.

To prevent the calculations of $M_1[v]$ and $M_2[u]$ from becoming prohibitively complicated, we will insist that the g's be chosen so that the ordering of any two terms that are subtracted in the calculations of $M_1[v]$ and $M_2[u]$ is fixed. Since we are trying to construct a four-parameter model that reduces to the two-parameter model, we choose the ordering to match that of the two-parameter model. From Table II, we see that

$$\begin{aligned}
&P_{1,1} - P_{1,2} \geqslant 0, \quad P_{1,3} - P_{1,4} \geqslant 0,\\
&P_{2,1} - P_{2,2} \leqslant 0, \quad P_{2,3} - P_{2,4} \leqslant 0,\\
&P_{3,1} - P_{3,2} \geqslant 0, \quad P_{3,3} - P_{3,4} \geqslant 0,\\
&P_{4,1} - P_{4,2} \leqslant 0, \quad P_{4,3} - P_{4,4} \leqslant 0,\\
&P_{1,2} - P_{1,4} \geqslant 0, \quad P_{1,1} - P_{1,3} \geqslant 0,\\
&P_{2,2} - P_{2,4} \geqslant 0, \quad P_{2,1} - P_{2,3} \geqslant 0,\\
&P_{3,2} - P_{3,4} \leqslant 0, \quad P_{3,1} - P_{3,3} \leqslant 0,\\
&P_{4,2} - P_{4,4} \leqslant 0, \quad P_{4,1} - P_{4,3} \leqslant 0.
\end{aligned} \tag{D42}$$

Note that in two cases ($P_{2,1} - P_{2,2}$ and $P_{4,3} - P_{4,4}$) these inequalities are inconsistent with Eqs. (D1), (D2), and (D4), but that is expected. Equations (D1), (D2), and (D4) are the conditions to saturate $S \leqslant 2 + M_2 + \hat{M}_1 + \hat{M}_2$, but for $M_2 + \hat{M}_1 + \hat{M}_2 > 2$, the bound to be saturated is $S \leqslant 4$. For these two cases, Table III shows that, for $M_2 + \hat{M}_1 + \hat{M}_2 \leqslant 2$, $P_{2,1} = P_{2,2}$ and $P_{4,3} = P_{4,4}$, so the orderings specified in Eq. (D42) do not require any changes in ordering as $M_2 + \hat{M}_1 + \hat{M}_2$ crosses the borderline at 2.

The other crucial requirement on the g's is the positivity of the conditional probabilities,

$$P_{i,j} \geqslant 0. \tag{D43}$$

With the orderings specified in Eq. (D42), it is straightforward to find

$$\begin{aligned} M_1[y] &= M_1 + 2(g_2 + g_5 - 2h), \\ M_2[x] &= M_2 + 2(g_1 + g_3 - 2h), \\ M_1[y'] &= \hat{M}_1 + 2(g_4 + g_7 - 2h), \\ M_2[x'] &= \hat{M}_2 + 2(g_6 + g_8 - 2h). \end{aligned} \tag{D44}$$

A successful model requires that the second term on the right-hand side of each line should vanish, which allows us to solve for g_5, g_3, g_7, and g_8 in terms of the other g's.

The problem now is to find values for the independent g_i's—g_1, g_2, g_4, and g_6—which are consistent with all the constraints in Eqs. (D42) and (D43).

When the 32 constraints are written out, one finds that each of the four independent g_i's appears in 8 of them, with 4 in the form of upper limits, and 4 in the form of lower limits. In every case there is one redundant pair, so each independent g_i has three upper bounds and three lower bounds. One of the upper bounds and one of the lower bounds involves a second independent g, so we put those bounds aside for later consideration. This leaves two upper bounds and two lower bounds for each independent g_i. Depending on parameters, either one of the upper bounds and either one of the lower bounds can be the most restrictive. One can then construct a function equal to the minimum of the two upper bounds and a function equal to the maximum of the two lower bounds, so now one has one upper bound and one lower bound for each independent g_i. It can then be shown that if these bounds are all satisfied, then the inequalities that we put aside—those that involve more than one independent g_i—are automatically satisfied.

By comparing the bounding functions for the different g_i's, one finds that there are some simple regularities. $g_{1,\max}$ is for all parameters at least as stringent as $g_{6,\max}$, so we can take $g_{1,\max}$ as the upper bound for both g_1 and g_6, where

$$\begin{aligned} g_{1,\max} = \tfrac{1}{16}[R + 4(2\hat{M}_1 + \hat{M}_2 + 2) \\ - 8\max(M_2 + \hat{M}_1, 2) + 4q_2], \end{aligned} \tag{D45}$$

where R and q_2 were defined in Eqs. (83) and (79), respectively. Similarly, we can take $g_{6,\min}$ as the lower bound for both g_1 and g_6, where

$$\begin{aligned} g_{6,\min} = \tfrac{1}{16}[R + 4(2 + \hat{M}_2) \\ - 8\min(\hat{M}_2 + M_1, 2) + 4q_2)]. \end{aligned} \tag{D46}$$

Since g_1 and g_6 now have the same upper and lower bounds, we can choose to satisfy these relations by setting them equal to each other, and equal to the mean of the upper and lower bounds:

$$g_1 = g_6 = \tfrac{1}{2}[g_{1,\max} + g_{6,\min}]. \tag{D47}$$

A similar analysis of g_2 and g_4 shows that they can also be described by common bounds, with

$$g_{2,\max} = \tfrac{1}{16}[-3R + 8(M_2 - 2) \tag{D48}$$

$$+ 8\min(M_1 + \hat{M}_2, 2) - 8q_2), \tag{D49}$$

$$g_{4,\min} = \tfrac{1}{16}[8\max(\hat{M}_1 + M_2, 2) - 3R - 16]. \tag{D50}$$

We choose the solution

$$g_2 = g_4 = \tfrac{1}{2}[g_{2,\max} + g_{4,\min}]. \tag{D51}$$

The final notation was chosen to simplify the appearance of the solution, defining

$$g_1 = g_6 = h - q_4, \tag{D52}$$

$$g_2 = g_4 = h + q_4, \tag{D53}$$

where q_4 was defined in Eq. (81).

When the matrix $G_{i,j}$ is rewritten in terms of q_3 and q_4, one finds the conditional probabilities given in Table IV, thus completing the construction of the four-parameter model.

[1] J. S. Bell, On the Einstein-Podolsky-Rosen paradox, Physics **1**, 195 (1964).

[2] J. F. Clauser, M. A. Horne, A. Shimony, and R. A. Holt, Proposed Experiment to Test Local Hidden-Variable Theories, Phys. Rev. Lett. **23**, 880 (1969).

[3] J. S. Bell, The theory of local beables, Epistemol. Lett. **9**, 86 (1976).

[4] J. S. Bell, J. F. Clauser, M. A. Horne, and A. Shimony, An exchange on local beables, Dialectica **39**, 85 (1985).

[5] J. S. Bell, *Speakable and Unspeakable in Quantum Mechanics* (Cambridge University Press, New York, 1987).

[6] B. Hensen, H. Bernien, A. E. Dréau, A. Reiserer, N. Kalb, M. S. Blok, J. Ruitenberg, R. F. L. Vermeulen, R. N. Schouten, C. Abellán, W. Amaya, V. Pruneri, M. W. Mitchell, M. Markham, D. J. Twitchen, D. Elkouss, S. Wehner, T. H. Taminiau, and R. Hanson, Loophole-free Bell inequality violation using electron spins separated by 1.3 kilometres, Nature (London) **526**, 682 (2015).

[7] L. K. Shalm, E. Meyer-Scott, B. G. Christensen, P. Bierhorst, M. A. Wayne, M. J. Stevens, T. Gerrits, S. Glancy, D. R. Hamel, M. S. Allman, K. J. Coakley, S. D. Dyer, C. Hodge, A. E. Lita, V. B. Verma, C. Lambrocco, E. Tortorici, A. L. Migdall, Y. Zhang, D. R. Kumor, W. H. Farr, F. Marsili, M. D. Shaw, J. A. Stern, C. Abellán, W. Amaya, V. Pruneri, T. Jennewein, M. W. Mitchell, P. G. Kwiat, J. C. Bienfang, R. P. Mirin, E. Knill, and S. W. Nam, Strong Loophole-Free Test of Local Realism, Phys. Rev. Lett. **115**, 250402 (2015).

[8] M. Giustina, M. A. M. Versteegh, S. Wengerowsky, J. Handsteiner, A. Hochrainer, K. Phelan, F. Steinlechner, J. Kofler, J.-Å. Larsson, C. Abellán, W. Amaya, V. Pruneri, M. W. Mitchell, J. Beyer, T. Gerrits, A. E. Lita, L. K. Shalm, S. W. Nam, T. Scheidl, R. Ursin, B. Wittmann, and A. Zeilinger, Significant-Loophole-Free Test of Bell's Theorem with Entangled Photons, Phys. Rev. Lett. **115**, 250401 (2015).

[9] B. Hensen, N. Kalb, M. S. Blok, A. E. Dréau, A. Reiserer, R. F. L. Vermeulen, R. N. Schouten, M. Markham, D. J.

Twitchen, K. Goodenough, D. Elkouss, S. Wehner, T. H. Taminiau, and R. Hanson, Loophole-free Bell test using electron spins in diamond: Second experiment and additional analysis, Sci. Rep. **6**, 30289 (2016).

[10] W. Rosenfeld, D. Burchardt, R. Garthoff, K. Redeker, N. Ortegel, M. Rau, and H. Weinfurter, Event-Ready Bell Test Using Entangled Atoms Simultaneously Closing Detection and Locality Loopholes, Phys. Rev. Lett. **119**, 010402 (2017).

[11] J. Handsteiner, A. S. Friedman, D. Rauch, J. Gallicchio, B. Liu, H. Hosp, J. Kofler, D. Bricher, M. Fink, C. Leung, A. Mark, H. T. Nguyen, I. Sanders, F. Steinlechner, R. Ursin, S. Wengerowsky, A. H. Guth, D. I. Kaiser, T. Scheidl, and A. Zeilinger, Cosmic Bell Test: Measurement Settings from Milky Way Stars, Phys. Rev. Lett. **118**, 060401 (2017).

[12] J. Yun, Y. Cao, Y.-H. Li, S.-K. Liao, L. Zhang, J.-G. Ren, W.-Q. Cai, W.-Y. Liu, B. Li, H. Dai, G.-B. Li, Q.-M. Lu, Y.-H. Gong, Y. Xu, S.-L. Li, F.-Z. Li, Y.-Y. Yin, Z.-Q. Jiang, M. Li, J.-J. Jia, G. Ren, D. He, Y.-L. Zhou, X.-X. Zhang, N. Wang, X. Chang, Z.-C. Zhu, N.-L. Liu, Y.-A. Chen, C.-Y. Lu, R. Shu, C.-Z. Peng, J.-Y. Wang, and J.-W. Pan, Satellite-based entanglement distribution over 1200 kilometers, Science **356**, 1140 (2017).

[13] C. Abellán *et al.* (The BIG Bell Test Collaboration), Challenging local realism with human choices, Nature (London) **557**, 212 (2018).

[14] D. Rauch, J. Handsteiner, A. Hochrainer, J. Gallicchio, A. S. Friedman, C. Leung, B. Liu, L. Bulla, S. Ecker, F. Steinlechner, R. Ursin, B. Hu, D. Leon, C. Benn, A. Ghedina, M. Cecconi, A. H. Guth, D. I. Kaiser, T. Scheidl, and A. Zeilinger, Cosmic Bell Test Using Random Measurement Settings from High-Redshift Quasars, Phys. Rev. Lett. **121**, 080403 (2018).

[15] M.-H. Li, C. Wu, Y. Zhang, W.-Z. Liu, B. Bai, Y. Liu, W. Zhang, Q. Zhao, H. Li, Z. Wang, L. You, W. J. Munro, J. Yin, J. Zhang, C.-Z. Peng, X. Ma, Q. Zhang, J. Fan, and J.-W. Pan, Test of Local Realism into the Past without Detection and Locality Loopholes, Phys. Rev. Lett. **121**, 080404 (2018).

[16] N. Brunner, D. Cavalcanti, S. Pironio, V. Scarani, and S. Wehner, Bell nonlocality, Rev. Mod. Phys. **86**, 419 (2014).

[17] J.-Å. Larsson, Loopholes in Bell inequality tests of local realism, J. Phys. A **47**, 424003 (2014).

[18] A. Aspect, J. Dalibard, and G. Roger, Experimental Test of Bell's Inequalities Using Time-Varying Analyzers, Phys. Rev. Lett. **49**, 1804 (1982).

[19] G. Weihs, T. Jennewein, C. Simon, H. Weinfurter, and A. Zeilinger, Violation of Bell's Inequality under Strict Einstein Locality Conditions, Phys. Rev. Lett. **81**, 5039 (1998).

[20] P. M. Pearle, Hidden-variable example based upon data rejection, Phys. Rev. D **2**, 1418 (1970).

[21] P. H. Eberhard, Background level and counter efficiencies required for a loophole-free Einstein-Podolsky-Rosen experiment, Phys. Rev. A **47**, R747 (1993).

[22] M. A. Rowe, D. Kielpinski, V. Meyer, C. A. Sackett, W. M. Itano, C. Monroe, and D. J. Wineland, Experimental violation of a Bell's inequality with efficient detection, Nature (London) **409**, 791 (2001).

[23] M. Ansmann, H. Wang, R. C. Bialczak, M. Hofheinz, E. Lucero, M. Neeley, A. D. O'Connell, D. Sank, M. Weides, J. Wenner, A. N. Cleland, and J. M. Martinis, Violation of Bell's inequality in Josephson phase qubits, Nature (London) **461**, 504 (2009).

[24] T. Scheidl, R. Ursin, J. Kofler, S. Ramelow, X. S. Ma, Th. Herbst, L. Ratschbacher, A. Fedrizzi, N. K. Langford, T. Jennewein, and A. Zeilinger, Violation of local realism with freedom of choice, Proc. Natl. Acad. Sci. USA **107**, 19708 (2010).

[25] J. Hofmann, M. Krug, N. Ortegel, L. Gérard, M. Weber, W. Rosenfeld, and H. Weinfurter, Heralded entanglement between widely separated atoms, Science **337**, 72 (2012).

[26] M. Giustina, A. Mech, S. Ramelow, B. Wittmann, J. Kofler, J. Beyer, A. Lita, B. Calkins, T. Gerrits, S. W. Nam, R. Ursin, and A. Zeilinger, Bell violation using entangled photons without the fair-sampling assumption, Nature (London) **497**, 227 (2013).

[27] B. G. Christensen, K. T. McCusker, J. B. Altepeter, B. Calkins, T. Gerrits, A. E. Lita, A. Miller, L. K. Shalm, Y. Zhang, S. W. Nam, N. Brunner, C. C. W. Lim, N. Gisin, and P. G. Kwiat, Detection-Loophole-Free Test of Quantum Nonlocality, and Applications, Phys. Rev. Lett. **111**, 130406 (2013).

[28] J. Barrett and N. Gisin, How Much Measurement Independence Is Needed to Demonstrate Nonlocality? Phys. Rev. Lett. **106**, 100406 (2011).

[29] D. E. Koh, M. J. W. Hall, Setiawan, J. E. Pope, C. Marletto, A. Kay, V. Scarani, and A. Ekert, Effects of Reduced Measurement Independence on Bell-Based Randomness Expansion, Phys. Rev. Lett. **109**, 160404 (2012).

[30] M. J. W. Hall, Local Deterministic Model of Singlet State Correlations Based on Relaxing Measurement Independence, Phys. Rev. Lett. **105**, 250404 (2010).

[31] M. J. W. Hall, Relaxed Bell inequalities and Kochen-Specker theorems, Phys. Rev. A **84**, 022102 (2011).

[32] M. Banik, M. Rajjak Gazi, S. Das, A. Rai, and S. Kunkri, Optimal free will on one side in reproducing the singlet correlation, J. Phys. A **45**, 205301 (2012).

[33] G. Pütz, D. Rosset, T. J. Barnea, Y.-C. Liang, and N. Gisin, Arbitrarily Small Amount of Measurement Independence Is Sufficient to Manifest Quantum Nonlocality, Phys. Rev. Lett. **113**, 190402 (2014).

[34] G. Pütz and N. Gisin, Measurement dependent locality, New J. Phys. **18**, 055006 (2016).

[35] C. H. Brans, Bell's theorem does not eliminate fully causal hidden variables, Int. J. Theor. Phys. **27**, 219 (1988).

[36] J. Kofler, T. Paterek, and Č. Brukner, Experimenter's freedom in Bell's theorem and quantum cryptography, Phys. Rev. A **73**, 022104 (2006).

[37] S. Weinstein, Nonlocality without nonlocality, Found. Phys. **39**, 921 (2009).

[38] L. P. Thinh, L. Sheridan, and V. Scarani, Bell tests with min-entropy sources, Phys. Rev. A **87**, 062121 (2013).

[39] J. E. Pope and A. Kay, Limited measurement dependence in multiple runs of a Bell test, Phys. Rev. A **88**, 032110 (2013).

[40] L. Vervoort, Bell's theorem: Two neglected solutions, Found. Phys. **43**, 769 (2013).

[41] B. Paul, K. Mukherjee, and D. Sarkar, One sided indeterminism alone is not a useful resource to simulate any nonlocal correlation, Quantum Inf. Process. **13**, 1687 (2014).

[42] J. Gallicchio, A. S. Friedman, and D. I. Kaiser, Testing Bell's Inequality with Cosmic Photons: Closing the Setting-Independence Loophole, Phys. Rev. Lett. **112**, 110405 (2014).

[43] R. Chaves, R. Kueng, J. B. Brask, and D. Gross, Unifying Framework for Relaxations of the Causal Assumptions in Bell's Theorem, Phys. Rev. Lett. **114**, 140403 (2015).

[44] D. Aktas, S. Tanzilli, A. Martin, G. Pütz, R. Thew, and N. Gisin, Demonstration of Quantum Nonlocality in the Presence of Measurement Dependence, Phys. Rev. Lett. **114**, 220404 (2015).
[45] S. Weinstein, Learning the Einstein-Podolsky-Rosen correlations on a restricted Boltzmann machine, arXiv:1707.03114.
[46] S. Weinstein, Neural networks as "hidden" variable models for quantum systems, arXiv:1807.03910.
[47] J. Barrett, L. Hardy, and A. Kent, No Signaling and Quantum Key Distribution, Phys. Rev. Lett. **95**, 010503 (2005).
[48] S. Pironio, A. Acín, N. Brunner, N. Gisin, S. Massar, and V. Scarani, Device-independent quantum key distribution secure against collective attacks, New J. Phys. **11**, 045021 (2009).
[49] U. Vazirani and T. Vidick, Fully Device-Independent Quantum Key Distribution, Phys. Rev. Lett. **113**, 140501 (2014).
[50] S. Pironio, A. Acín, S. Massar, A. B. de La Giroday, D. N. Matsukevich, P. Maunz, S. Olmschenk, D. Hayes, L. Luo, T. A. Manning, and C. Monroe, Random numbers certified by Bell's theorem, Nature (London) **464**, 1021 (2010).
[51] R. Colbeck and R. Renner, Free randomness can be amplified, Nat. Phys. **8**, 450 (2012).
[52] R. Gallego, L. Masanes, G. de la Torre, C. Dhara, L. Aolita, and A. Acín, Full randomness from arbitrarily deterministic events, Nat. Commun. **4**, 2654 (2013).
[53] C. Wu, B. Bai, Y. Liu, X. Zhang, M. Yang, Y. Cao, J. Wang, S. Zhang, H. Zhou, X. Shi, X. Ma, J.-G. Ren, J. Zhang, C.-Z. Peng, J. Fan, Q. Zhang, and J.-W. Pan, Random Number Generation with Cosmic Photons, Phys. Rev. Lett. **118**, 140402 (2017).
[54] C. Leung, A. Brown, H. Nguyen, A. S. Friedman, D. I. Kaiser, and J. Gallicchio, Astronomical random numbers for quantum foundations experiments, Phys. Rev. A **97**, 042120 (2018).
[55] Y. Liu, X. Yuan, M.-H. Li, W. Zhang, Q. Zhao, J. Zhong, Y. Cao, Y.-H. Li, L.-K. Chen, H. Li, T. Peng, Y.-A. Chen, C.-Z. Peng, S.-C. Shi, Z. Wang, L. You, X. Ma, J. Fan, Q. Zhang, and J.-W. Pan, High-Speed Device-Independent Quantum Random Number Generation without a Detection Loophole, Phys. Rev. Lett. **120**, 010503 (2018).
[56] Y. Liu, Q. Zhao, M.-H. Li, J.-Y. Guan, Y. Zhang, B. Bai, W. Zhang, W.-Z. Liu, C. Wu, X. Yuan, H. Li, W. J. Munro, Z. Wang, L. You, J. Zhang, X. Ma, J. Fan, Q. Zhang, and J.-W. Pan, Device-independent quantum random-number generation, Nature (London) **562**, 548 (2018).
[57] P. Bierhorst, E. Knill, S. Glancy, Y. Zhang, A. Mink, S. Jordan, A. Rommal, Y.-K. Liu, B. Christensen, S. W. Nam, M. J. Stevens, and L. K. Shalm, Experimentally generated randomness certified by the impossibility of superluminal signals, Nature (London) **556**, 223 (2018).
[58] L. Shen, J. Lee, L. P. Thinh, J.-D. Bancal, A. Cerè, A. Lamas-Linares, A. Lita, T. Gerrits, S. W. Nam, V. Scarani, and C. Kurtsiefer, Randomness Extraction from Bell Violation with Continuous Parametric Down-Conversion, Phys. Rev. Lett. **121**, 150402 (2018).
[59] X. Yuan, Z. Cao, and X. Ma, Randomness requirement on the Clauser-Horne-Shimony-Holt Bell test in the multiple-run scenario, Phys. Rev. A **91**, 032111 (2015).
[60] X. Yuan, Q. Zhao, and X. Ma, Clauser-Horne Bell test with imperfect random inputs, Phys. Rev. A **92**, 022107 (2015).
[61] D.-D. Li, Y.-Q. Zhou, F. Gao, X.-H. Li, and Q.-Y. Wen, Effects of measurement dependence on generalized Clauser-Horne-Shimony-Holt Bell test in the single-run and multiple-run scenarios, Phys. Rev. A **94**, 012104 (2016).
[62] E. Y.-Z. Tan, Y. Cai, and V. Scarani, Measurement-dependent locality beyond independent and identically distributed runs, Phys. Rev. A **94**, 032117 (2016).
[63] Y. Teng, S. Yang, S. Wang, and M. Zhao, Tight bound on randomness for violating the Clauser-Horne-Shimony-Holt inequality, IEEE Trans. Inf. Theory **62**, 1748 (2016).
[64] M. J. W. Hall, The significance of measurement independence for Bell inequalities and locality, in *At the Frontier of Spacetime*, edited by T. Asselmeyer-Maluga (Springer, Switzerland, 2016), Chap. 11, p. 189.
[65] J. Degorre, S. Laplante, and J. Roland, Simulating quantum correlations as a distributed sampling problem, Phys. Rev. A **72**, 062314 (2005).
[66] C. Branciard, N. Brunner, N. Gisin, C. Kurtsiefer, A. Lamas-Linares, A. Ling, and V. Scarani, Testing quantum correlations versus single-particle properties within Leggett's model and beyond, Nat. Phys. **4**, 681 (2008).
[67] B. F. Toner and D. Bacon, Communication Cost of Simulating Bell Correlations, Phys. Rev. Lett. **91**, 187904 (2003).
[68] H. M. Wiseman, The two Bell's theorems of John Bell, J. Phys. A **47**, 424001 (2014).
[69] O. Costa De Beauregard, S-matrix, Feynman zigzag and Einstein correlation, Phys. Lett. A **67**, 171 (1978).
[70] N. Argaman, Bell's theorem and the causal arrow of time, Am. J. Phys. **78**, 1007 (2010).
[71] H. Price and K. Wharton, Disentangling the quantum world, Entropy **17**, 7752 (2015).
[72] J. Conway and S. Kochen, The free will theorem, Found. Phys. **36**, 1441 (2006).
[73] G. 't Hooft, The free-will postulate in quantum mechanics, arXiv:quant-ph/0701097.
[74] Michael A. Nielsen and Isaac L. Chuang, *Quantum Computation and Quantum Information* (Cambridge University Press, Cambridge, 2010).
[75] C. A. Fuchs and J. van de Graaf, Cryptographic distinguishability measures for quantum-mechanical states, IEEE Trans. Inf. Theory **45**, 1216 (1999).
[76] B. S. Cirel'son, Quantum generalizations of Bell's inequality, Lett. Math. Phys. **4**, 93 (1980).
[77] S. Hossenfelder, Testing super-deterministic hidden variables theories, Found. Phys. **41**, 1521 (2011).
[78] S. Hossenfelder, The free will function, arXiv:1202.0720.
[79] S. Hossenfelder, Testing superdeterministic conspiracy, J. Phys.: Conf. Ser. **504**, 012018 (2014).
[80] G. 't Hooft, The emergence of quantum mechanics, in *Frontiers of Fundamental Physics: The Eleventh International Symposium*, edited by J. Kouneiher, C. Barbachoux, T. Masson, and D. Vey, AIP Conf. Proc. No. 1446 (AIP, Melville, NY, 2012) p. 341
[81] G. 't Hooft, *The Cellular Automaton Interpretation of Quantum Mechanics* (Springer, New York, 2016).
[82] G. 't Hooft, Physics on the boundary between classical and quantum mechanics, J. Phys.: Conf. Ser. **504**, 012003 (2014).
[83] G. 't Hooft, Relating the quantum mechanics of discrete systems to standard canonical quantum mechanics, Found. Phys. **44**, 406 (2014).

[84] G. 't Hooft, Free will in the theory of everything, arXiv:1709.02874.

[85] D. M. Greenberger, M. A. Horne, A. Shimony, and A. Zeilinger, Bell's theorem without inequalities, Am. J. Phys. **58**, 1131 (1990).

[86] N. D. Mermin, Simple Unified Form for the Major No-Hidden-Variables Theorems, Phys. Rev. Lett. **65**, 3373 (1990).

[87] A. S. Friedman, D. I. Kaiser, and J. Gallicchio, The shared causal pasts and futures of cosmological events, Phys. Rev. D **88**, 044038 (2013).